AEROSPACE NUCLEAR SAFETY

# RESEARCH REPORT

## RE-ENTRY FLIGHT DEMONSTRATION NUMBER ONE (RFD-1): FINAL SNAP-10A SAFETY FLIGHT-TEST PLAN

Department 7410

SC-RR-64-501
TID-4500 (27th Edition)
AEROSPACE SAFETY

SANDIA CORPORATION

PRIME CONTRACTOR TO THE
UNITED STATES ATOMIC
ENERGY COMMISSION
ALBUQUERQUE, NEW MEXICO
LIVERMORE, CALIFORNIA

## DISCLAIMER

TID-4500 (27th Edition)
AEROSPACE SAFETY

SC-RR-64-501

# RE-ENTRY FLIGHT DEMONSTRATION NUMBER ONE (RFD-1):

# FINAL SNAP-10A SAFETY FLIGHT-TEST PLAN

PREPARED BY:

C. E. Erickson, 7413-1
J. I. Hegge, 7412-2
J. Jacobs, 7412-2
R. D. Klett, 7412-2
H. R. Spahr, 7412-2
H. K. Togami, 7412-2
I. B. White, 7411

REVIEWED BY:

C. E. Erickson, 7413-1
H. E. Hansen, 7411
A. J. Clark, Jr., 7412
A. E. Bentz, 7413

APPROVED BY:

V. E. Blake, 7410
D. B. Shuster, 7400

ABSTRACT

This report constitutes the RFD-1 Safety Flight Plan for investigating the disassembly, destruction, and disposal of the SNAP-10A reactor during re-entry. The re-entry test vehicle on which the inert reactor is mounted will be placed in the re-entry trajectory by a NASA Scout launched from Wallops Island, Virginia. Launched at 90 degrees elevation along a 129-degree heading, the Scout trajectory will be programmed to guide the test vehicle into a flight path passing near Bermuda at 150,000 feet altitude, with impact occurring approximately 150 miles south of Bermuda. Telemetry, optical, and radar coverage will be used to gather data describing the behavior of the test vehicle and the SNAP-10A reactor during re-entry into the atmosphere from 400,000 feet altitude. (This report, although published after the actual flight, is confined to matters relating to the flight-test plan as it existed prior to March 1963.)

Report date: March 1963

Publication date: March 1964

ACKNOWLEDGMENT

Sandia Corporation Department 7410, Aerospace Nuclear Safety Department, acknowledges the outstanding support of the following Sandia Corporation Organizations without whose help the RFD-1 flight and subsequent analysis could not have been performed:

| Organization Number | Organization Name | Organization Number | Organization Name |
|---|---|---|---|
| 1110 | Materials & Process Department I | 3400 | Technical Information & Publications |
| 1120 | Materials & Process Department II | 4200 | Development Shops |
| 1320 | Electromechanical Development Department I | 4300 | Purchasing |
| 1330 | Electromechanical Development Department II | 4410 | Design Definition Department |
| 1420 | Electronic Systems Department | 4500 | Plant Engineering & Maintenance |
| 1430 | Electronic Components Department | 5410 | Nuclear Burst Physics Department |
| 1440 | Reliability Department | 7210 | Test Projects Department |
| 1530 | Systems Engineering Department | 7220 | Test Range Department |
| 1540 | Engineering Analysis Department | 7240 | Test Support Department |
| 2640 | Engineering & Research Support Department | 7250 | Nuclear Test Department |
| 3210 | Safety Engineering Department | 7320 | Environmental Research & Operations Department |
| 3240 | Security Standards & Operations Department | 7330 | Planning & Functional Test Department |
| 3300 | Medical | 7420 | Aero- & Thermodynamics Department |
| | | 7430 | Space Projects Department |
| | | 7620 | Programming Department |

In addition to the encouragement and support given by the Division of Reactor Development of the AEC, Sandia Corporation gratefully acknowledges the support of Atomics International (AI), the National Aeronautics and Space Administration (NASA), the United States Air Force (USAF), the United States Coast Guard (USCG), and the United States Navy (USN) in the performance of the RFD-1 flight program. Other organizations contributing to this program are acknowledged by specific references to their support throughout the text of this report.

Issued by Sandia Corporation,
a prime contractor to the
United States Atomic Energy Commission



Printed in USA. Price $1.75. Available from the Office of Technical Services, Department of Commerce, Washington 25, D.C.

## FOREWORD

Sandia Corporation, a prime nuclear weapon contractor to the AEC, was authorized by the Division of Reactor Development to act as the prime contractor for the independent safety evaluation of aerospace nuclear power systems. The Aerospace Nuclear Safety program at Sandia includes research and development studies, ground testing, flight testing, systems analysis, and independent safety assessment. Re-entry Flight Demonstration Number 1 is the first re-entry flight test to be conducted since the initiation of this program in March 1962.

The SNAP-10A reactor (Systems for Nuclear Auxiliary Power) was selected for the first re-entry safety flight test. The selection of the SNAP-10A reactor, designed and constructed by Atomics International (AI), was based upon its proposed early use in a nuclear auxiliary power supply for earth satellites.

In the application of nuclear energy to space vehicles, safety features are designed into the power supplies to preclude significant hazards to the earth's population during aborted missions or orbital-decay re-entries.

The Safety Flight Test, called Re-entry Flight Demonstration Number One (RFD-1), employed an inert version of the SNAP-10A reactor to determine the effectiveness of the safety design. The simulated reactor was mounted to a re-entry vehicle (RV), which was placed into the required trajectory by a four-stage NASA Scout booster launched from Wallops Island, Virginia.

Sandia Corporation carried out its assignment in the Aerospace Nuclear Safety Program by performing the following tasks:

1. Design of the flight-test experiment and of the configuration of the simulated reactor, in cooperation with Atomics International.
2. Study of the capabilities of the Scout launch vehicle, and recommendation of a trajectory to assure that the desired information would be obtained.
3. Design of the re-entry vehicle (including telemetry system) and coordination of interface problems with Atomics International, NASA, and Ling Temco Vought Corporation.
4. Theoretical predictions of flight-test results.
5. Preparation of support requirements documents for the Atlantic Missile Range (AMR) and for the NASA stations at Wallops and Bermuda.
6. Provision of complementary downrange instrumentation for collecting telemetry and optical data.
7. Management of flight implementation activities.
8. Data reduction and analysis.
9. Comparison of flight-test results with theoretical calculations.

The following Sandia Corporation reports, together with the present volume, comprise the final documentation of Re-entry Flight Demonstration Number One (RFD-1):

SC-RR-64-502: Re-Entry Flight Demonstration Number One (RFD-1): Data Book

SC-RR-64-510: Re-Entry Flight Demonstration Number One (RFD-1): Comparison of the Pre-Flight and Observed Trajectories

SC-RR-64-511: Re-Entry Flight Demonstration Number One (RFD-1): Design, Development, and Performance of the Re-Entry Vehicle

SC-RR-64-515: Re-Entry Flight Demonstration Number One (RFD-1): Pre-Flight Disassembly Analysis and Observed Disassembly of the Simulated SNAP-10A Reactor

SC-RR-64-516: Re-Entry Flight Demonstration Number One (RFD-1): Optical Data and Fuel Element Experiment

SC-RR-64-517: Re-Entry Flight Demonstration Number One (RFD-1): Atmospheric Sciences Support

TABLE OF CONTENTS


| | Page |
|---|---|
| SECTION I -- INTRODUCTION | 7 |
| SECTION II -- TEST OBJECTIVES AND LIMITATIONS | 10 |
| A. Discussion | 10 |
| B. Re-entry Heating Disassembly | 10 |
| C. Fuel Rod Ablation | 10 |
| SECTION III -- FLIGHT OPERATIONS PLAN | 12 |
| A. Launch and Trajectory (See Figures 4 and 5) | 12 |
| B. Telemetry Coverage | 13 |
| C. Optical Coverage (See Section VI for Details) | 13 |
| D. Radar Tracking | 14 |
| E. Recovery | 14 |
| F. Meteorological Support | 14 |
| SECTION IV -- FLIGHT-TEST CONFIGURATION | 15 |
| A. Discussion of Re-entry System | 15 |
| B. Reactor Detail | 16 |
| C. Discussion of Re-entry Vehicle | 20 |
| D. Re-entry Vehicle Shell Detail | 20 |
| E. Motor Ejection System Detail | 22 |
| F. Recovery System Detail | 23 |
| G. External Fuel Rods | 23 |
| H. Launch Vehicle | 24 |
| SECTION V -- FLIGHT-TEST PARAMETERS | 26 |
| A. Discussion | 26 |
| B. Scout Trajectory | 28 |
| C. Re-entry System Trajectory | 29 |
| D. External Fuel Rod Trajectory | 34 |
| E. Predicted Sequence of Events | 35 |
| SECTION VI -- VEHICLE AND RANGE INSTRUMENTATION | 36 |
| A. Re-entry System Telemetry | 36 |
| B. SARAH | 47 |
| C. Flashing Light Beacon | 47 |
| D. Range Instrumentation | 47 |
| SECTION VII -- GROUND TESTS | 49 |
| A. Qualification Tests | 49 |
| B. Acceptance Tests | 54 |
| SECTION VIII -- SCHEDULE | 55 |
| SECTION IX -- ORGANIZATION RESPONSIBILITIES - JWG | 56 |
| SECTION X -- WALLOPS RANGE DESCRIPTION | 57 |
| A. General | 57 |
| B. Definition | 57 |
| C. Purpose | 57 |
| D. Range Capability | 57 |
| E. Geography | 57 |
| F. Downrange Stations | 58 |
| G. Bermuda | 58 |
| H. Instrumentation | 58 |

TABLE OF CONTENTS (cont)


| | | Page |
|---|---|---|
| APPENDIX -- SCOUT RE-ENTRY STUDY CONDUCTED FOR SANDIA CORPORATION | | 63 |


TABLES


| Table | | |
|---|---|---|
| I | Re-entry System Weight as a Function of Altitude | 30 |
| II | Drag Coefficient as a Function of Mach Number | 30 |
| III | RFD-1 Telemetry Components - Airborne | 40 |
| IV | RFD-1 Telemetry Channel Allocations | 41 |
| V | Telemetry | 41 |
| VI | Telemetry | 42 |


LIST OF ILLUSTRATIONS


| Figure | | |
|---|---|---|
| 1 | SNAP-10A | 7 |
| 2 | SNAP-10A reactor | 8 |
| 3 | Desired SNAP-10A orbital decay re-entry sequence | 9 |
| 4 | SNAP-10A safety flight-test trajectory | 12 |
| 5 | Predicted Wallops-to-Bermuda flight path | 12 |
| 6 | Impact dispersion and downrange stations | 13 |
| 7 | Layout drawing of RFD-1 with fourth-stage motor | 17 |
| 8 | Model of re-entry system, fourth-stage motor (X-248) and ascent heat shield | 19 |
| 9 | RFD-1 re-entry system | 19 |
| 10 | Cross-section plan of re-entry vehicle | 21 |
| 11 | Sectional view of fuel element with tracer | 24 |
| 12 | Scout vehicle configuration | 25 |
| 13 | Comparison of RFD-1 theoretical orbital decay with predicted trajectory without parachute | 27 |
| 14 | Comparison of heating for RFD-1 predicted re-entry and theoretical orbital decay | 27 |
| 15 | Nominal trajectory prediction for Scout S-116 | 29 |
| 16 | RS trajectory and heating | 31 |
| 17 | Re-entry event sequence as function of range | 32 |
| 18 | RS trajectory and heating as functions of time | 32 |
| 19 | RS trajectory as function of time (includes parachute descent) | 33 |
| 20 | External fuel rod trajectory and heating | 34 |
| 21 | External fuel rod heating | 34 |
| 22 | TM package | 36 |
| 23 | TM package | 37 |
| 24 | TM package | 37 |
| 25 | TM package | 38 |
| 26 | TM block diagram | 39 |
| 27 | Antenna pattern coordinate system (telemetry) | 43 |
| 28 | TM antenna pattern | 44 |
| 29 | Antenna pattern coordinate system (beacon) | 45 |
| 30 | C-band antenna pattern | 45 |
| 31 | Block diagram of pyrotechnic circuitry | 46 |
| 32 | Temperature cycling test, RS without TM package | 49 |
| 33 | Temperature cycling test, RS with TM package | 50 |
| 34 | Requested radiant heat inputs for first full-scale unit | 51 |
| 35 | Requested radiant heat inputs for second full-scale unit | 51 |
| 36 | Radiant heat input for nose cone test | 52 |
| 37 | Requested radiant heat input for flare | 52 |
| 38 | RFD-1 test schedule | 55 |
| 39 | Wallops Station, overall site map | 59 |

## SECTION I -- INTRODUCTION

This report is the first of a series comprising the final documentation of Re-entry Flight Demonstration Number One (RFD-1). As was explained in the Foreword to this volume, RFD-1 will be the first re-entry flight test of an inert reactor for a nuclear auxiliary power supply. For this test the SNAP-10A reactor, designed and constructed by Atomics International (AI), was selected because it is the first reactor-type nuclear auxiliary power supply scheduled for use with satellites.

The SNAP-10A (Figure 1) utilizes a thermoelectric energy conversion system to deliver 500 watts of electrical power for one year of operation in space. A reflector-controlled nuclear reactor (Figure 2) provides the heat source; a eutectic mixture of sodium-potassium (NaK-78) is used to transfer heat from the core to the thermoelectric junctions.

After operating in space at normal power for one year, the SNAP-10A will contain a long-lived fission product inventory within its core which will necessitate disposing of the core in a manner to preclude any significant hazard to the earth's population. The design goal is to provide a configuration which will allow the core to burn up from the heating associated with orbital decay re-entry. The proposed re-entry burnup of the core should result in particle sizes small enough to allow sufficient decay and dispersion during fallout to preclude intolerable atmospheric or ground contamination.

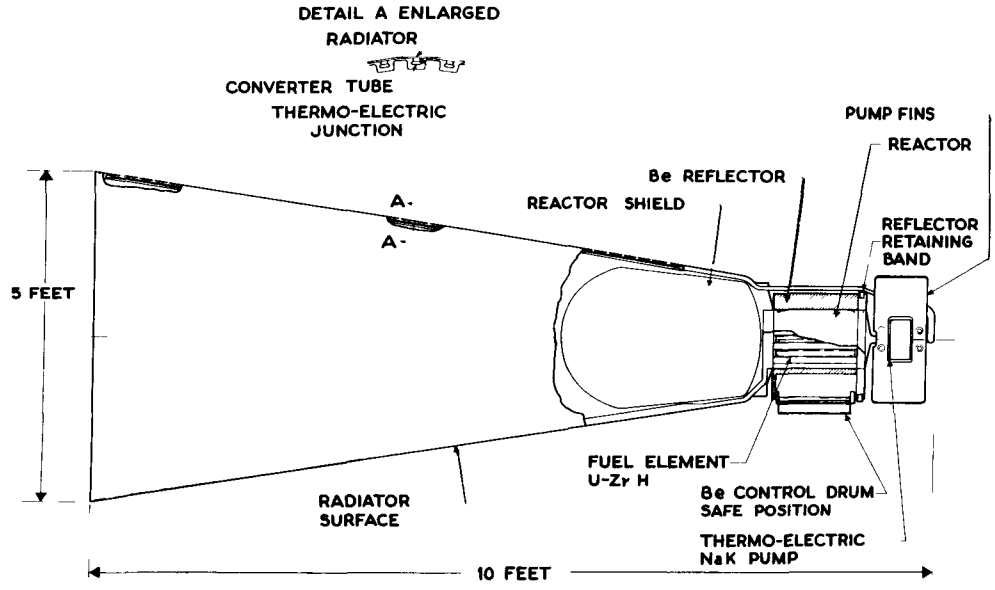


Figure 1. SNAP-10A

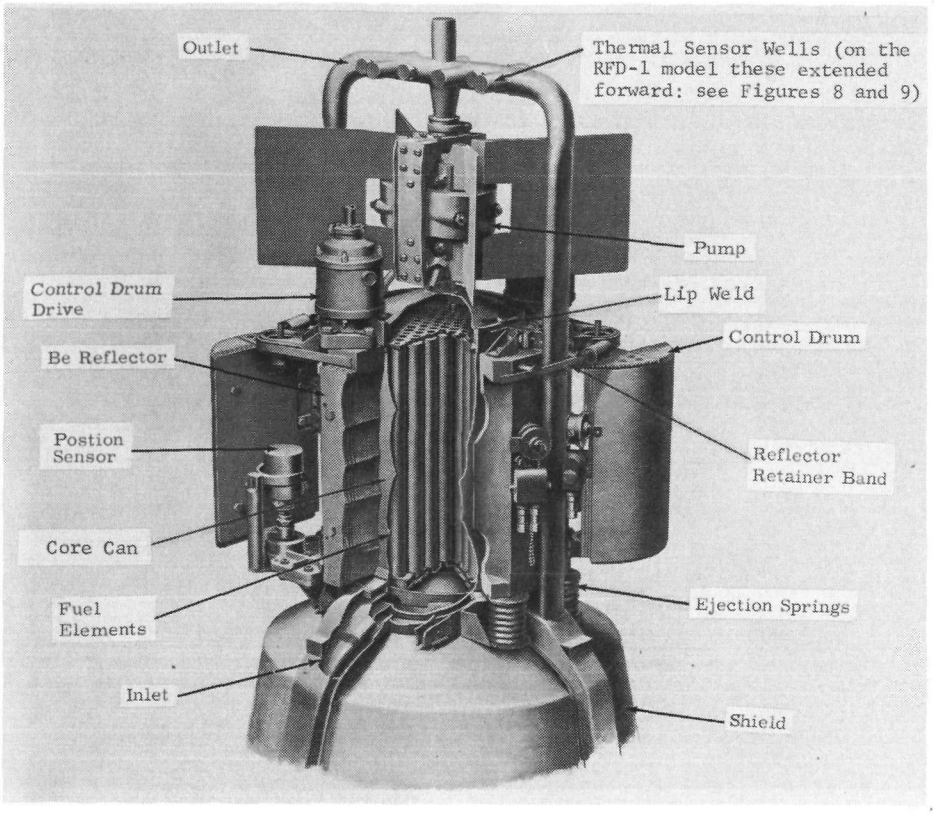


Figure 2. SNAP-10A reactor

The design adopted by Atomics International for the SNAP-10A to ensure safe re-entry of the system includes certain mechanical disassembly features to allow early exposure of the reactor core to re-entry heating. The sequence necessary to expose the core involves:

1. Separation of the fusible link to allow ejection, by springs, of the beryllium reflector assembly
2. Burnoff of the NaK pipe and pump radiator
3. Melting of the core can lid and sides
4. Release of the fuel elements from the can.

Figure 3 shows the desired sequence of events during orbital decay.

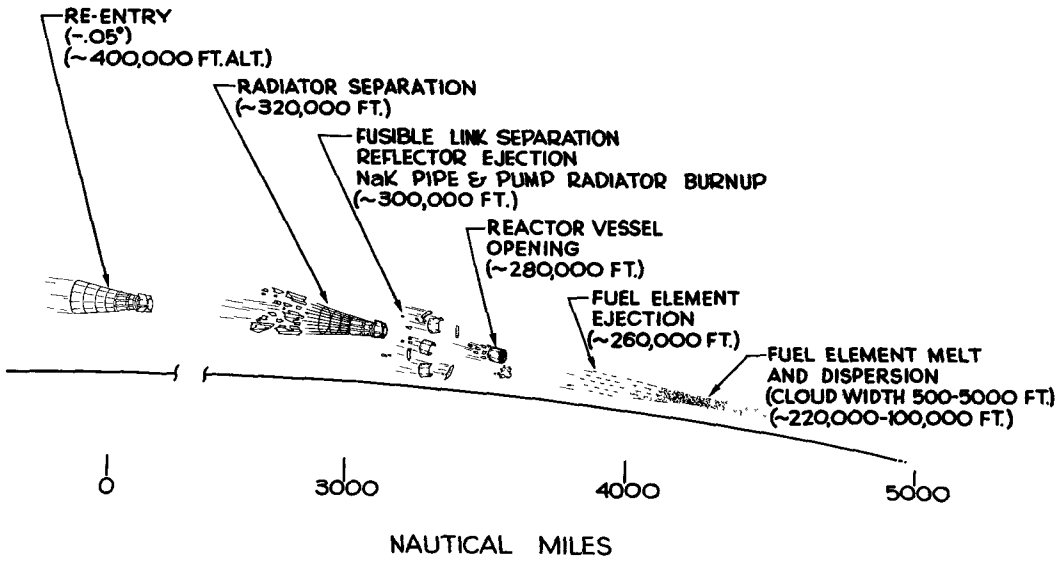


Figure 3. Desired SNAP-10A orbital decay re-entry sequence

The purposes of RFD-1 are to determine the effectiveness of mechanical disassembly during re-entry and to obtain experimental burnup data to compare with theoretical predictions. Telemetry, optical, and radar coverage will be employed to accomplish these purposes. In addition, to allow visual observation of the effects of re-entry heating on the re-entry system and on the fixed fuel rods attached to the base of the reactor, recovery will be attempted. The arrangements are considered in more detail in the Sections which follow.

## SECTION II -- TEST OBJECTIVES AND LIMITATIONS

### A. Discussion

In an ideal test, the entire power supply would be simulated by an inert model, and the complete sequence listed above in Section I would be verified by an actual orbital decay re-entry. However, because of obvious difficulties in controlling and instrumenting such a flight, and because of limitations in time and money, RFD-1 will entail compromised flight parameters (Section V) to test re-entry heating disassembly and fuel rod ablation. Because of limitations discussed in Section IV-B, the test reactor will contain no fuel elements. Instead, 12 simulated fuel rods will be flown external to the RS (Re-entry System) and ejected early in the trajectory to allow at least partial burnup at the -6 degree re-entry angle of this test (see Sections IV-G and V-D). Three fixed fuel rods mounted at the base of the reactor are discussed under Reactor Instrumentation in Section IV-B.

### B. Re-entry Heating Disassembly

Disassembly is the basis on which safe re-entry of SNAP-10A is predicated, since only if this occurs will the fuel elements be exposed to heating early enough in the re-entry trajectory to allow complete burnup. Therefore, the primary objectives of RFD-1 are to provide experimental verification of the effectiveness of the reactor disassembly design and to obtain data to support theoretical calculations on burnup. To attain these objectives, the reactor has been extensively instrumented with switches and thermocouples. The latter will measure the temperature at points determined by analysis to be vital to burnup of the assembly; the switches are located so as to signal ejection of the reflector and disassembly of the core can.

### C. Fuel Rod Ablation

The safety of SNAP-10A may depend on complete ablation and dispersion of the UZrH fuel rods. Knowledge of the response of UZrH to the environment of re-entry into the atmosphere is very limited. Calculations indicate that, for orbital decay re-entry, aerodynamic heating alone is probably insufficient to ensure complete ablation of the SNAP-10A fuel elements. This heating effect, however, may be small compared to the exothermic chemical reactions of uranium, zirconium, and hydrogen with the re-entry atmosphere. Exact simulation of the re-entry environment by laboratory experiments is not possible. Therefore, it has been decided to include a fuel rod ablation experiment on the RFD-1 flight test. This experiment has the following objectives:

1. To obtain data, for UZrH in general and SNAP-10A fuel rods in particular, on ablation rate and volume consumed by burnup during re-entry
2. To confirm theoretical calculations and predictions on re-entry burnup
3. To evaluate optical instrumentation techniques for use in future flight tests.

To attain these objectives, fuel rods containing various tracer elements have been designed; these are described in detail in Section IV-G. The experiment concept is to eject simultaneously four groups of three rods each early during re-entry and then record their burnup with spectral, plate, and motion picture cameras. (See Section VI-D.) Since all the rods will follow the same trajectory and experience essentially the same heating, the UZrH should ablate away first from the group of

rods with the least wall thickness, thus exposing the tracer element contained in that group. The tracer will then burn, emitting a flare characteristic of the element. Because wall thickness varies among the groups of rods, each tracer element will flare at a different time and altitude. Comparison of rod volume and time of element burnup with the calculated heating for the trajectory will provide indications of the rate and volume of ablation versus re-entry heating.

## SECTION III -- FLIGHT OPERATIONS PLAN

### A. Launch and Trajectory (See Figures 4 and 5)

The RFD-1 payload will be placed in its re-entry trajectory by a Scout vehicle launched from Wallops Island. At launch, RFD-1 telemetry information will be received and recorded at the Wallops Main Base Telemetry Station. Because of the optical coverage required, launch will be attempted only during periods of maximum darkness, defined as no moonlight and no twilight.

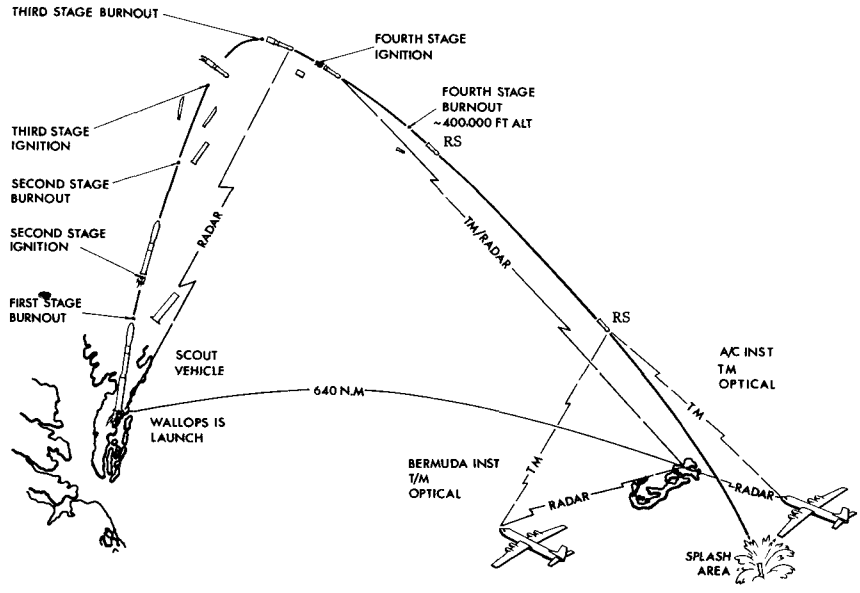


Figure 4.

SNAP-10A safety flight-test trajectory

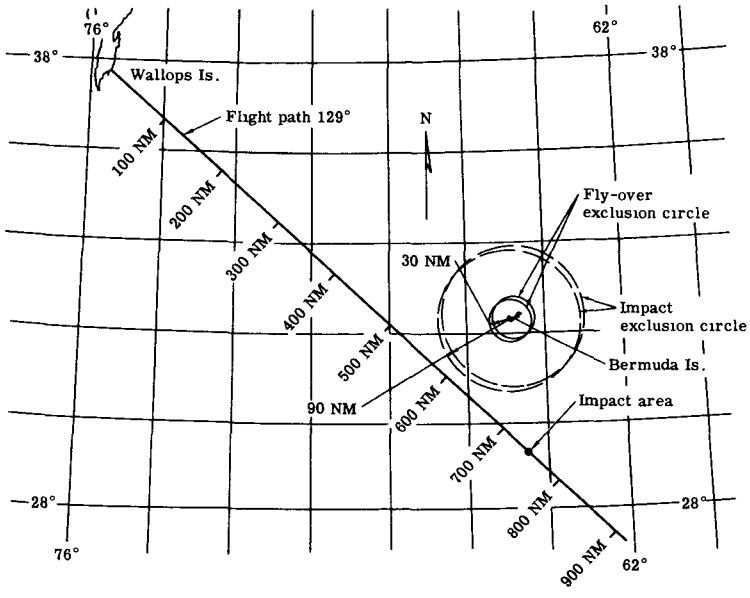


Figure 5.

Predicted Wallops-to-Bermuda flight path

The Scout will be launched at 90° elevation with a heading 129° in azimuth and will be programmed to provide a re-entry angle of -6° ± 1° at 400,000 feet, with the further requirement that the re-entry system (RS) pass Bermuda at an altitude of 150,000 feet (see Section V for details).

B. Telemetry Coverage

1. Ground - Wallops Main Base Telemetry and the Bermuda Mercury Station will record the received signal.

2. Aircraft - AFSWC will provide, and Sandia will instrument, two C-54 aircraft downrange to record telemetry. AFMTC will provide one (perhaps two) JC-130A aircraft at the impact area; they will be equipped to record the received telemetry signal.

3. Ship - The NASA Range Recoverer (from Wallops) and an AFMTC ORV (Ocean Range Vessel) will be stationed near the impact area to record telemetry.

Aircraft and ship deployment will be approximately as shown in Figure 6.

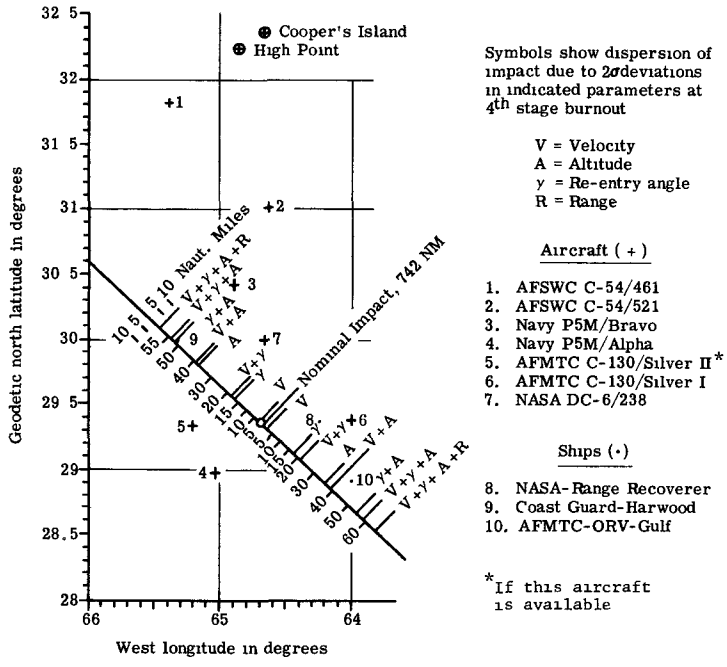


Figure 6.

Impact dispersion and downrange stations

C. Optical Coverage (See Section VI for Details)

1. Ground - The re-entry will be tracked by Sandia equipment installed at Bermuda.

2. Aircraft - The two C-54 aircraft mentioned above will also have cameras to record the visual events during re-entry.

D. Radar Tracking

The FPS-16 radar at Bermuda will be used to track the re-entry system which includes a C-band transponder (beacon) to aid in acquisition and tracking at maximum distance.

E. Recovery

Included in the re-entry system is a parachute to reduce impact velocity, and, to aid in locating the RS, a flashing light beacon and a SARAH beacon. Both C-54 aircraft, the AFMTC JC-130A aircraft, and both the NASA Range Recoverer and ORV ships will be equipped to receive the SARAH signal. In addition, a Navy P5M aircraft and a minesweeper will be stationed at the impact area to monitor the SARAH signal and assist in the actual recovery operation. All of the ships will be equipped to perform the actual recovery of the RS.

F. Meteorological Support

1. Wallops Island -- Since Wallops Island will be concerned with atmospheric conditions affecting the Scout vehicle, standard balloon runs will be made to determine winds aloft; local conditions affecting the safety of launch will also be monitored.

2. Bermuda -- To obtain data on high altitude winds and air density, Sandia and NASA will fire six small sounding rockets in groups of three. The first three will be fired as soon as possible after the RFD-1 impact and the second group will be fired 12 hours later. Each group will consist of a Sandia Kisha-Judi rocket with densitometer, a Sandia Deacon-Judi rocket with chaff, and a NASA Arcas sounding rocket.

## SECTION IV -- FLIGHT-TEST CONFIGURATION

### A. Discussion of Re-entry System

For the purposes of this test plan, the term "Re-entry System" (RS) designates the flight configuration, consisting of a SNAP-10A inert reactor test configuration attached to a Sandia-designed re-entry vehicle (RV). Note that the RV does not include the inert reactor. Figures 7 and 8 (pp. 17-19) show the re-entry system, fourth-stage engine, and the 34-inch Scout heat shield in the launch configuration. The re-entry system alone is shown in Figure 9 (p. 19).

Complicating factors in the design and development of the RFD-1 re-entry system were:

1. Stringent volume and weight limitations imposed by the Scout launch vehicle and its heat shield
2. An early launch date, requiring tightly scheduled design, development, and testing efforts
3. Requirements to build the RV around the fourth-stage motor and still attain an adequately stable aerodynamic shape; and to maintain an acceptable center-of-gravity location by ejecting the fourth-stage motor after its burnout
4. Severe aerodynamic heating inputs to the RS
5. A complex reactor shape, making burnup analysis difficult
6. Large changes in RS shape, weight, center of gravity, and aerodynamic coefficients during re-entry, resulting from reactor burnup and RV ablation.

The re-entry system design was initiated by a theoretical study to select the most stable RV shape compatible with the Scout heat-shield requirements. Once this shape had been selected and defined, layouts and RS design were commenced; and computations were initiated on trajectories based on theoretical aerodynamic coefficients.

To determine more realistic aerodynamic coefficients for stability analysis and trajectory calculations, aerodynamic force tests were conducted on scale models of the re-entry system for several stages of reactor disassembly. These tests were performed in the Sandia transonic (Mach 0.5 to 3.0) and hypersonic (Mach 7) wind tunnels and in the Cornell Aeronautical Laboratory 40-inch shock tunnel (Mach 11 to 20). Aerodynamic heating tests were conducted on full-scale and quarter-scale models in the Arnold Engineering Development Center (AEDC) 100-inch hot-shot facility (Mach 17 to 21) to determine heating inputs to the RS. The quarter-scale model was later tested in the Rhodes and Bloxsom 60-inch hot-shot tunnel. This test corroborated the results of the AEDC test, and served to familiarize Sandia with the capabilities of the facility and the technique of using a special temperature-sensitive paint to obtain aerodynamic heat-transfer data.

Subsequently, structural RV components were designed and tested as described in detail in Part D of this Section. Theoretical stress calculations were made for the RS for Scout launch loads and re-entry loads, based on calculated RS time-temperature curves.

Design and fabrication of two RFD-1 qualification re-entry systems included the reactor modifications discussed below in B, and the RV design changes dictated by the development tests. These two units were subjected to the following design

qualification tests to qualify for the Scout launch and re-entry conditions (described in detail in Section VII):

1. Temperature cycling
2. Vibration
3. Linear acceleration
4. Temperature shock
5. Spin
6. Mechanical shock
7. Acoustical noise
8. Radiant heat
9. Telemetry and antenna checkout.

Both design qualification units successfully passed all these tests.

Based on the results of the design qualification tests, two RFD-1 RS flight units have been built, and have passed the following acceptance tests (described in Section VII):

1. Temperature cycling
2. Vibration
3. Spin
4. Telemetry and antenna checkout.

The second unit is considered a backup unit for the launch.

## B. Reactor Detail

The RFD-1 payload consists of a full-scale SNAP-10A reactor mockup fabricated and instrumented by Atomics International. By joint agreement between AI and Sandia, the reactor-RV interface and instrumentation requirements were defined, and the required deviations from an operational SNAP-10A reactor were determined. Actual SNAP-10A reactor parts have been used wherever possible, with the following exceptions:

1. The beryllium reflectors and control drums have been replaced by aluminum components designed to exactly simulate the originals in shape and in clearance from the core can. Payload weight limitations on the Scout launch vehicle require this weight reduction modification. Further, this replacement precludes the possibility of BeO hazards from burnup or ablation of the beryllium parts. These aluminum reflectors and drums are, however, provided with actual SNAP-10A hinges, ejection springs, and fusible link band.

2. The NaK coolant has been omitted from the system to reduce weight, to prevent the large NaK flare from obscuring the tracer material in the external fuel rod experiment, and to help prevent extension of the duration of RF blackout. During actual orbital decay, the NaK line will burn off early in re-entry, thereby permitting the NaK to escape. Absence of the NaK is calculated to affect heat transfer rates by 0.5 to 6.0 percent, depending on the conditions.

3. The fuel rod complement and internal beryllium reflector have also been removed from the core can, since theoretical studies show that their removal will not appreciably affect heat transfer to the core can. Theoretical studies further indicate that, for the RFD-1 trajectory, the core can will not have burned sufficiently to permit the fuel rods to separate from it until the altitude has decreased to approximately 120,000 feet. (These studies were based on measured heat inputs to (a) a full-scale reactor tested in the 100-inch hot-shot tunnel of the AEDC (Arnold Engineering Development Company), and (b) a core can tested in the Sandia radiant heat facility.) Even with the core can burned sufficiently, aerodynamic forces would prevent separation of the fuel rods until an even lower altitude, and the aerodynamic heating encountered would be insufficient to yield information on fuel rod burnup.

The elimination of the internal fuel rods made it necessary to include the external fuel-rod experiment on RFD-1.

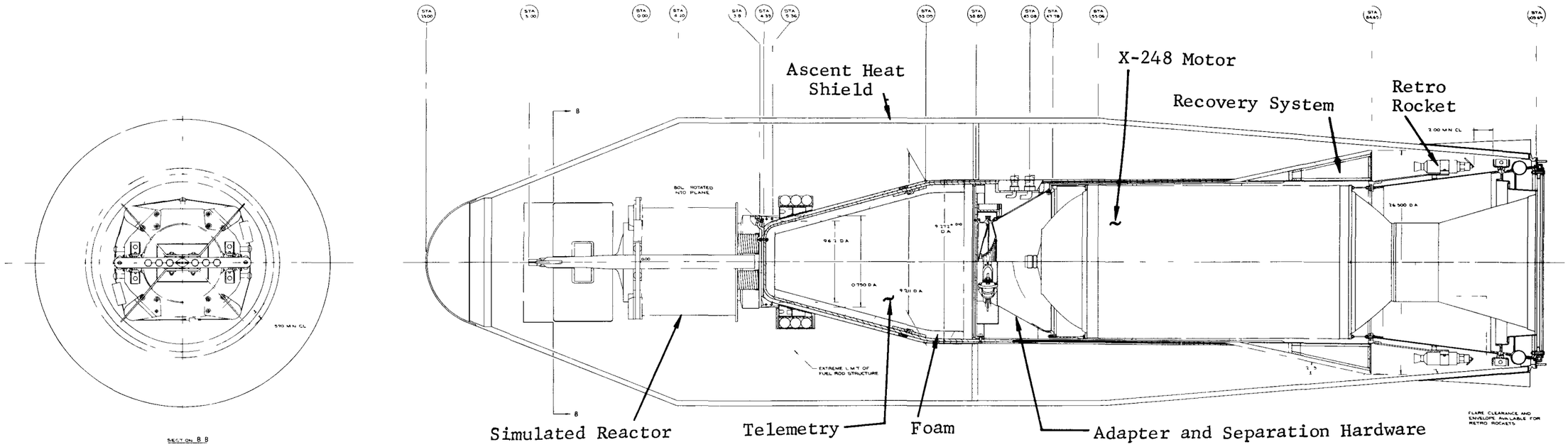


Figure 7. Layout drawing of RFD-1 with fourth stage motor

BLANK

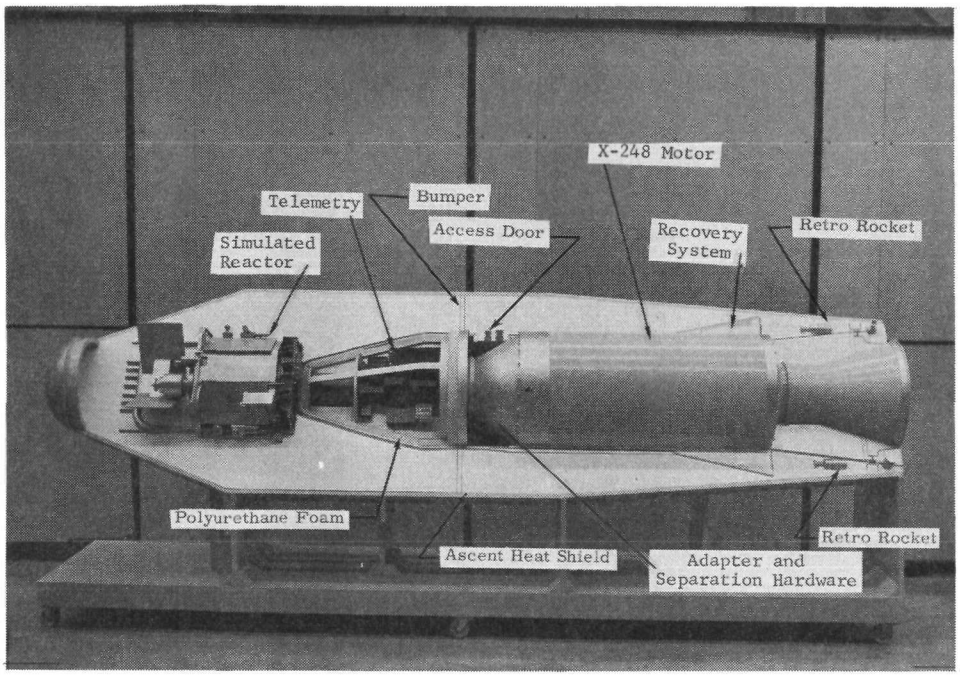


Figure 8. Model of re-entry system, fourth stage motor (X-248) and ascent heat shield

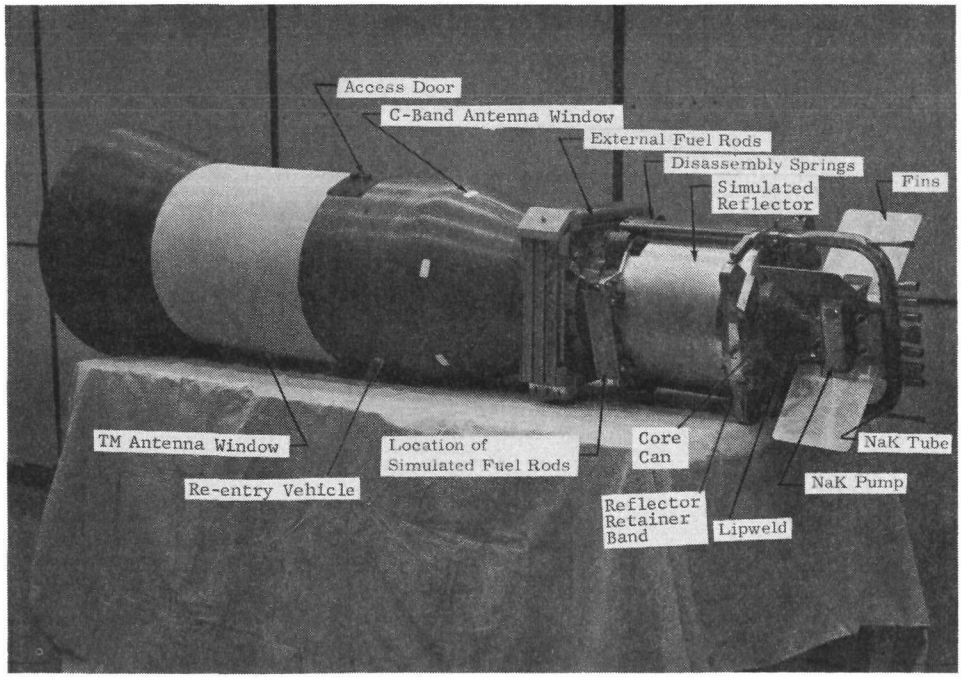


Figure 9. RFD-1 re-entry system

Reactor Instrumentation -- The reactor has a total of 20 thermocouples mounted at the following locations: the fusible band, the band support, the band weld, the band standoff, the fins, the NaK tube, the base of the NaK pump, the lip weld, and the core vessel wall. Another themocouple is mounted in a heat meter attached to the base of the reactor. This heat meter consists of a thermocouple embedded in a copper slug. The copper slug in turn is encased in an aluminum oxide ceramic cylinder 1-1/4 inch in diameter and 1-1/4 inch long (outside dimensions). The heat meter is necessary to measure the heat input at this location, where three simulated fuel rods are also mounted. Two of the rods (simulated SNAP-10A fuel) measure 1-1/4 inch in diameter by 1-1/4 inch long, while a third (simulated Rover fuel) measures only 1/2 inch in diameter by 1-1/4 inch long. So located, the fuel rods will not interfere with the main objective of investigating reactor disassembly. An attempt will be made to recover these fuel rods after the flight in order to study them for the effects of re-entry ablation.

In addition to the thermocouples for temperature measurements, six switches are mounted to monitor ejection of the reflector and disassembly of the core vessel.

Four instrumented reactor mockups have been fabricated by AI. Two were used in the two re-entry systems which went through the design qualification tests, and two are being used in the two flight re-entry systems.

Reactor instrumentation performed satisfactorily before, during, and after each of the design qualification tests. The reflector ejection sequence was checked on one of the design qualification reactors after qualification tests were completed. When the fusible link band was heated with a torch to the approximate predicted temperature, its fusible links melted, and the reflectors ejected satisfactorily.

## C. Discussion of Re-entry Vehicle

The re-entry vehicle is designed to:

1. Provide support for the reactor and internal fuel rod experiment
2. Provide thermal protection for the telemetry package and antennas
3. Provide an aerodynamically stable shape to prevent tumbling of the reactor
4. Eject the fourth-stage motor after burnout
5. Eject a parachute to decelerate the RS before water impact
6. Provide a gas-filled bag for flotation, and aids to recovery after impact.

The major systems of the RV are the shell, the motor ejection system, the recovery system, and the external fuel-rod experiment.

## D. Re-entry Vehicle Shell Detail

Important considerations in the design of the re-entry vehicle shell were:

1. High re-entry heating inputs
2. Weight limitations
3. Limited time scale for design, development, and fabrication.

After the exterior shape of the shell had been fixed by a theoretical aerodynamic study, the materials, fabrication techniques, and design of certain critical areas of the RV were tested. This testing was conducted in the plasma jet and radiant heat facility at Sandia to simulate the heating rates expected during re-entry. The thickness of the ablation material was determined by theoretical calculations made on the Sandia thermalog (passive analog computer). Although early

studies were based on theoretical aerodynamic heating rates, final calculations used the heat inputs measured in the AEDC 100-inch hot-shot tunnel tests.

Figure 10 presents a section through the RV shell, showing some details of its construction. As with most current re-entry structures, this RV is made up of an outer ablation shell, a layer of insulation, and the support structure. Two differences from other RV shells are that the support structure acts as insulation, and that the support structure and ablation material are made as a single unit because of the similarity in thermal expansion of the two materials and the use of the same resin in both parts. This integral design simplified manufacture, reduced weight, and eliminated the need for a flexible bond between the ablation material and the support structure. Since RF is severely attenuated by charred phenolic-fiberglass, clean ablating Teflon was used for thermal protection over the telemetry and C-band antenna areas. Because of the higher thermal expansion of Teflon, a cored RTV-11 bond was required to attach the Teflon antenna windows to the case. For the window over the TM antenna, a phenolic-fiberglass retaining sleeve was bonded with FM-1000 over the forward edge of the Teflon to maintain a smooth transition surface and prevent aerodynamic forces from loosening the Teflon. A phenolic-fiberglass mount for attaching the reactor was provided on the forward end of the RV. The fiberglass provides adequate thermal protection for the instrumentation cables from the reactor through the nose of the RV.

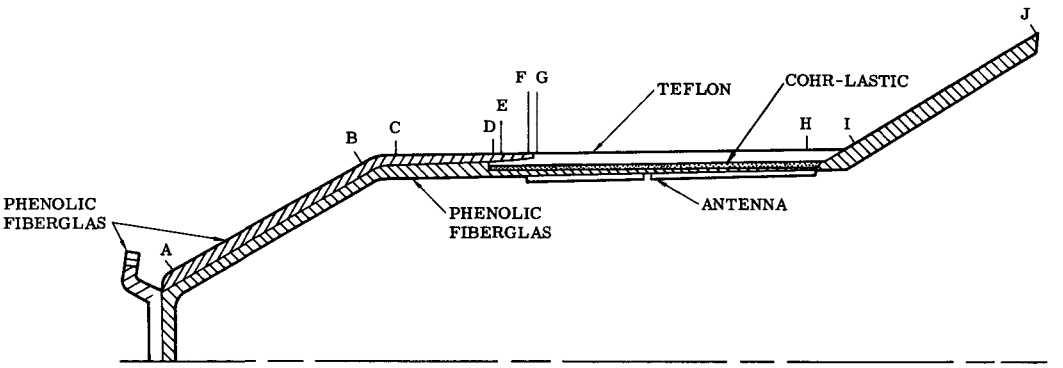


MATERIAL THICKNESS (INCHES)

| STATION | A | B | C | D | E | F | G | H | I | J |
|---|---|---|---|---|---|---|---|---|---|---|
| OUTER PHENOLIC-FIBERGLAS | 0.41 | 0.28 | 0.19 | 0.13 | 0.13 | 0.05 | | | | |
| BOND | 0.01 | 0.01 | 0.01 | 0.01 | 0.01 | 0.01 | | | | |
| INNER PHENOLIC-FIBERGLAS | 0.24 | 0.26 | 0.25 | 0.25 | 0.12 | 0.12 | 0.12 | 0.12 | 0.46 | 0.46 |
| TEFLON | -- | -- | -- | -- | 0.05 | 0.12 | 0.18 | 0.12 | -- | -- |
| COHR-LASTIC AND BOND | -- | -- | -- | -- | 0.08 | 0.08 | 0.08 | 0.08 | -- | -- |
| TOTAL | 0.66 | 0.55 | 0.45 | 0.39 | 0.39 | 0.38 | 0.38 | 0.32 | 0.46 | 0.46 |

Figure 10. Cross-section plan of re-entry vehicle

Six RV shells were fabricated. Two were used in development testing, two were used for design qualification tests, and two are the actual flight units. To determine the adequacy of the design, the development shells were subjected to the following tests:

1. Temperature shock
2. Vibration
3. Static loading
4. Linear acceleration
5. Radiant heat
6. Water entry

The changes suggested by the results of these tests were incorporated into the design qualification and flight units.

Thin coatings of Thermolag and D-65 were applied to the interior surface of the TM antenna, the parachute cavity cover, the 0.04-inch fiberglass liner, and the internal surface of the flare area.

To obtain information on re-entry shell ablation during flight, two ablation sensors, at different depths, were installed at two locations on the vehicle nose between points A and B of Figure 10. To determine the heat input to the RV nose cone, two copper heat meters, using chromel-alumel thermocouples, have also been installed in this location.

## E. Motor Ejection System Detail

Ejection of the fourth-stage motor from the RV is required to obtain a re-entry system center of gravity that will render the system aerodynamically stable. Important factors in the design of the ejection system were:

1. requirements for a simple system with proven reliability, and
2. limitations on space and weight.

The separation device was designed to serve as the structural link between the fourth-stage motor of the Scout launch vehicle and the re-entry system. The separation system consists of a motor adapter, a coil spring between the motor adapter and the re-entry system structure, a Marmon clamp with explosively actuated nuts, which holds the re-entry system structure to the motor adapter, and two 1-KS 40 Atlantic Research Corporation retrorockets.

The motor adapter was machined from AZ-31A-H24 magnesium to minimize weight. The coil spring supplies energy (35 ft-lb) to separate the fourth-stage motor from the RV. Retrorockets, which are initiated through electronic timers that delay ignition of the rockets until the fourth-stage motor has cleared the RV, will force the fourth-stage motor into a trajectory different from that of the RV. Retrorockets are necessary because outgassing of the fourth-stage motor produces an appreciable residual thrust. This thrust decays exponentially from a peak of approximately 12 pounds at the end of main burning to a value of about 2 pounds, 20 seconds later. Outgassing thrust decay continues down to approximately 0.8 pound at 280 seconds and remains approximately constant at this value for the next 520 seconds. The retrorockets will retard the fourth-stage motor after it has been ejected, and prevent a collision with the RS which could be caused by this residual thrust.

Reliability tests have been conducted on all pyrotechnic devices used in the RS. During the development tests, a separation test of a motor mockup from an RV mockup was made successfully during free fall from a drop tower. Actual motor cases, with ballast equivalent to the weight of the rocket nozzle, were ejected from re-entry vehicles dropped from an AD-5 (now designated as A1G) aircraft to check the recovery systems. After a few minor design changes, reliable ejection of the motor from the RV was consistently demonstrated on the last three re-entry vehicles dropped at Wallops Island.

The first flight unit underwent system checks before shipment to Wallops Island and also before installation on the Scout launch vehicle. During these tests, the pyrotechnic devices or simulated pyrotechnic devices were ignited, using the on-board timer and power supply, to verify proper system functioning. The second (backup) flight unit was subjected to limited system checks and will not be installed in a Scout vehicle unless it must be flown.

On the RFD-1, the external fuel-rod experiment and the motor separations are programmed to occur at the same time. As a result of theoretical study, 350,000 feet was chosen as the optimum altitude for these events to occur. At this altitude, the fuel rods will not have experienced any appreciable heating, and the firing of only one retrorocket will prevent the residual thrust from making the motor impact the RS.

## F. Recovery System Detail

The requirment for recovery was added after the initiation of the re-entry vehicle design. Important factors affecting the design of the recovery system were as follows:

1. The extremely small volume available for the recovery system
2. The necessity of placing most of the recovery system in the flare portion of the shell. Since this requirement tended to move the CG of the RS rearward, the recovery system weight had to be kept down to prevent an adverse CG location.

The recovery system includes a solid canopy parachute, a drogue gun, a flotation bag, two gas bottles, a flashing light, a dye marker, a Search and Recovery and Homing (SARAH) beacon, and a whip antenna. The operation of the 7-foot-diameter, solid canopy-type parachute was tested by aircraft drop tests and sled tests on the Sandia track. The parachute will be reefed at the skirt with a 2-foot line to reduce loads at parachute deployment. The drogue gun is a gun-type device for deploying the parachute by firing a steel slug. The gas bottles are thermally insulated to prevent a large buildup in pressure from re-entry heating. The SARAH beacon is a highly shock-resistant (in excess of 100 g) unit transmitting on a frequency of 235 mc through a Sandia-designed whip antenna erected at the time of parachute deployment.

The recovery system is designed so that, at an altitude of approximately 20,000 feet, two barometric switches, or backup timer signals from the TM package, will simultaneously fire the drogue gun and the gas-bottle explosive squib. Firing the drogue gun will eject the parachute cavity cover, deploy the parachute, and energize the flashing light. Ejection of the parachute cover will allow the SARAH beacon antenna to extend. Deployment of the parachute will initiate three Holex pyrotechnic cutters to cut the reefing line 10 seconds after deployment. Firing the explosive squib will permit the compressed $CO_2$ from the gas bottles to inflate the flotation bag to fill the cavity created by the ejected fourth-stage motor. The parachute decelerates the velocity of the RS from approximately 700 fps to approximately 100 fps at water impact, at which time the SARAH beacon is connected to its mercury battery power source by two salt-water switches or by an impact deceleration switch wired in parallel. After water impact, the RS floats in a nearly vertical position with approximately the rear third of its length extending above the water.

All phases of the operation of the recovery system and of ejection of the fourth-stage motor were tested in a series of drop tests from an A1G aircraft at the Sandia Tonopah ground range and at the NASA Wallops Island sea range. In the early tests, a timer and power supply replaced the telemetry. In the later tests, a special drop test TM system was used to telemeter recovery system operations to the ground. In the last drop test of the series, an actual RFD-1 flight TM system was used in the RV, with ejection of the fourth-stage motor added to the operation of the recovery system.

All pyrotechnic devices in the RS successfully passed the reliability tests. All nonhazardous RS components were included in the qualification and acceptance tests. The qualification tests, acceptance tests, sled tests, and aircraft drop tests were used to qualify the recovery system for the Scout launch and re-entry environment.

## G. External Fuel Rods

Calculations indicate that, for the RFD-1 trajectory, melting of the reactor core can lid and subsequent separation of the fuel rods will occur late in the flight. Consequently, it has been decided to mount the fuel rods externally on the RV so that their release into the atmosphere can be predetermined and independent of reactor events. The mounting and location are shown in Figure 9 (p. 19). The

rods will be released from the mounting by explosive bolts actuated by the timer in the telemetry system. The wires to the fuel rod mount will be severed by an explosive wire cutter to permit all the mount hardware to fall free after release.

To achieve the test objectives, it is necessary to measure the rate and volume of the ablation of the fuel rods as they burn during re-entry. The requirements for optical tracking dictate the design of the experimental rods. The configuration of the fuel rods is shown in Figure 11. There are four different groups of three rods with identical external dimensions. Internal dimensions and included tracers are as follows:

| Group | Wall Thickness | Tracer |
|---|---|---|
| 1 | 0.106 | Strontium |
| 2 | 0.184 | Barium |
| 3 | 0.306 | Silver |
| 4 | 0.406 | Gold |

These tracer materials were selected because of their strong and readily identified spectral lines. A 0.100-inch layer of fiberfrax insulation around the tracers is necessary to maintain them below their boiling points until the UZrH cylinder ablates away. The vent holes shown prevent any pressure buildup within the fuel elements. Alumina plugs are sprayed into the ends. This method of sealing has been selected because of the extreme difficulty of machining UZrH. The Hastelloy N cladding and external dimensions are exactly similar to the actual SNAP-10A fuel elements. Lead ballast in the strontium and barium rods is necessary to keep the $W/C_DA$ (ballistic coefficient) of the four rod groups similar so they will all follow the same re-entry trajectory.

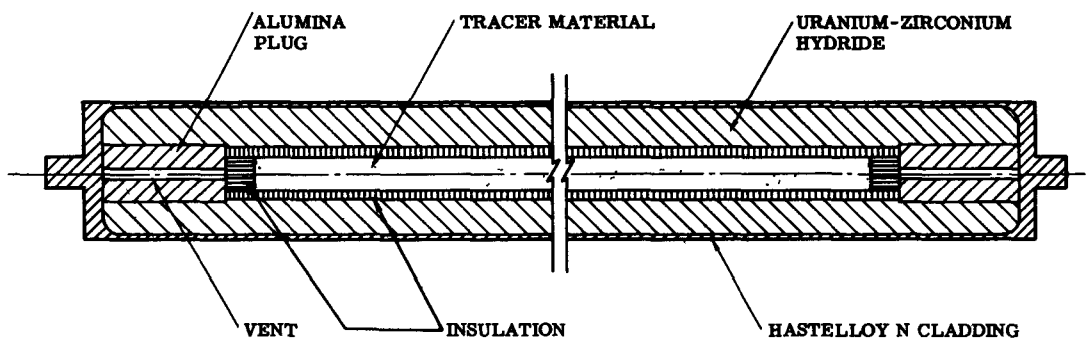


Figure 11. Sectional view of fuel element with tracer

During design and fabrication of the flight-test elements, in order to check the effects of including the tracers, (on ablation rate and structural integrity), a number of simulated rods were tested in a plasma jet facility. (This also will provide a reference for postflight check of the optical instrumentation.) Results verified the adequacy of the design and supplied insight about the probable ablation sequence. Details of this test were published in Reference 1.

## H. Launch Vehicle

The NASA four-stage solid-propellant Scout vehicle has been selected as the RFD-1 launch vehicle since it most nearly meets all the requirements of this program. Moreover, NASA has had considerable experience with the Scout, since it has been used for many flight tests, some of which have been similar to the planned RFD-1.

The RFD-1 Scout will be equipped with a 34-inch heat shield and will use the following motors:

First stage - Algol IIA
Second stage - Castor I
Third stage - Antares X-259-A2
Fourth stage - Altar X-248-A6

Figure 12 shows the Scout configuration with the RFD-1 payload installed. (For further details on the Scout launch vehicle, see Reference 2.)

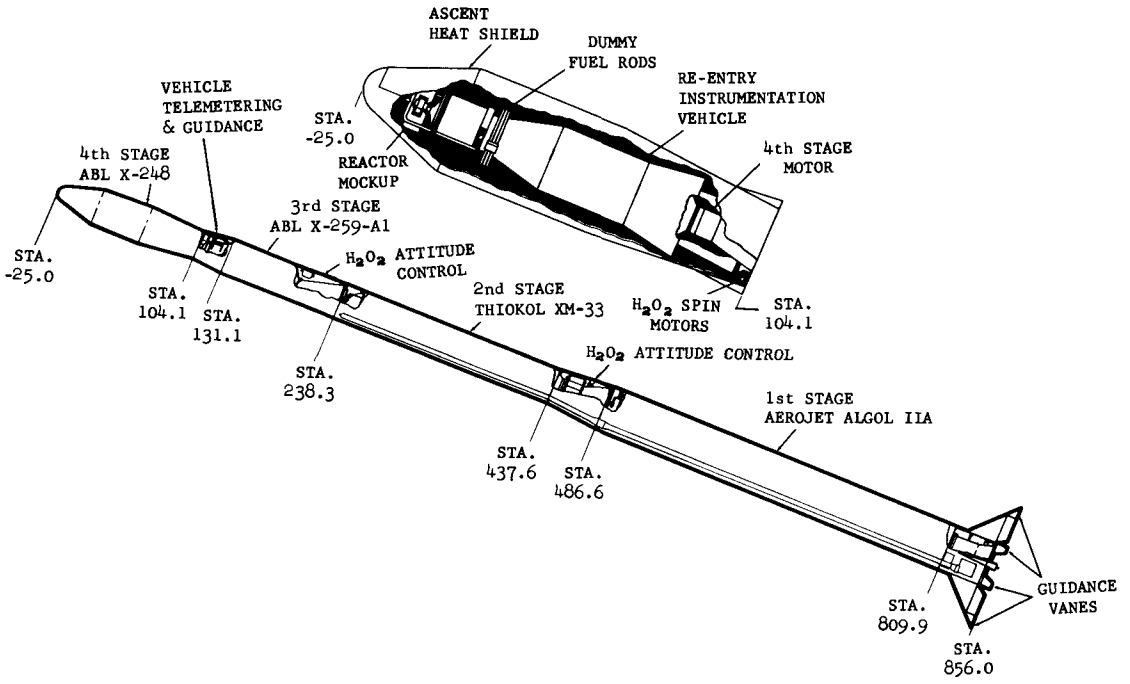


Figure 12. Scout vehicle configuration

## SECTION V -- FLIGHT-TEST PARAMETERS

### A. Discussion

To accomplish the objectives of this flight test the following conditions must be met:

1. The flight must result in the re-entry of a full-scale SNAP-10A reactor mockup, attached to a re-entry vehicle and instrumented to investigate reactor disassembly and burnup resulting from re-entry aerodynamic heating.

2. Simulated SNAP-10A fuel rods must be ejected from the RV at high altitude to permit investigation of burnup resulting from re-entry aerodynamic heating.

3. The re-entry velocities must be near orbital.

4. The re-entry angle must be as shallow as possible, consistent with range and instrumentation limitations and with launch vehicle guidance accuracy.

5. The re-entry burnup portion of the trajectory must occur near an island suitable for installation of ground-based instrumentation, including radar, telemetry receivers, and optical equipment.

6. All radioactive reactor components must be simulated, using non-radioactive materials, to preclude radiation hazards.

7. Recovery of the SNAP-10A re-entry system should be attempted in order to permit visual evaluation of the reactor, the attached fuel samples, and the RV after re-entry.

As was stated previously, an actual orbital decay of the RS (reactor and RV) would be desirable. Lacking this, the heating environment of orbital decay must be simulated as closely as possible. Acceptance of certain compromises were dictated, however, by the following requirements and conditions:

1. An early flight test (early in 1963)
2. A reliable launch vehicle with proven performance and ready availability
3. A limited budget
4. Limited downrange instrumentation.

The RFD-1 mission is defined as the launch, by a four-stage NASA Scout, of a SNAP-10A re-entry system from Wallops Island, Virginia, on a trajectory having a shallow re-entry angle with impact occurring in an area southeast of Bermuda. Figure 4 (p. 12) is a pictorial representation of the RFD-1 launch and trajectory. Figure 5 (p. 12) is a plan view of the flight path, while Figure 6 (p. 13) presents an enlarged view of the re-entry and impact portions of the flight.

A comparison of the RFD-1 trajectory with an orbital decay of the RFD-1 configuration is presented in Figure 13 and Figure 14 for the RS configuration that is to be flown. The orbital decay used in these figures is for an RFD-1 configuration, since a mission for the actual SNAP-10A has not been defined.

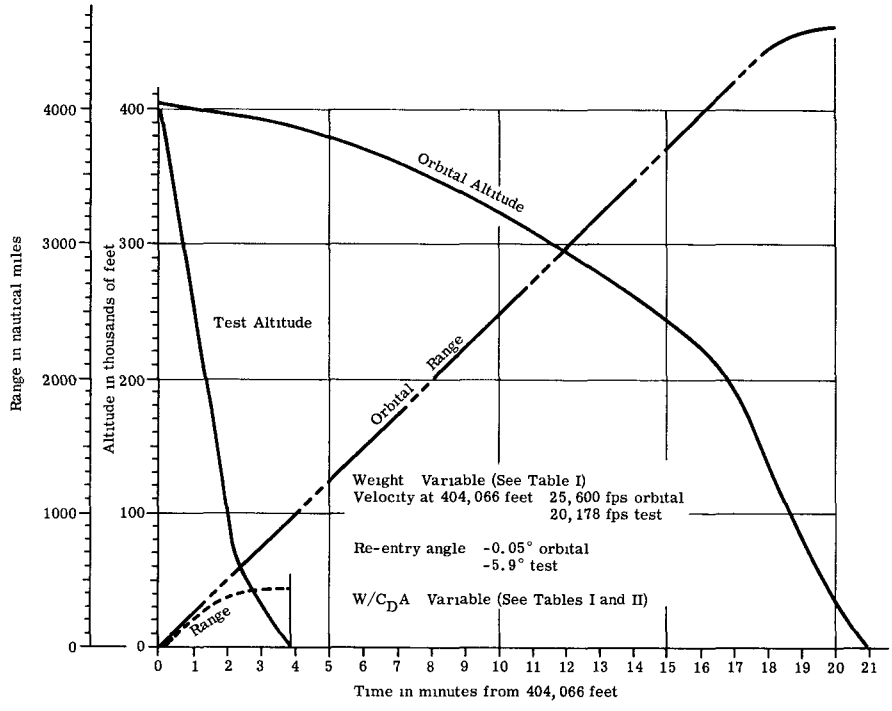


Figure 13. Comparison of RFD-1 theoretical orbital decay with predicted trajectory without parachute

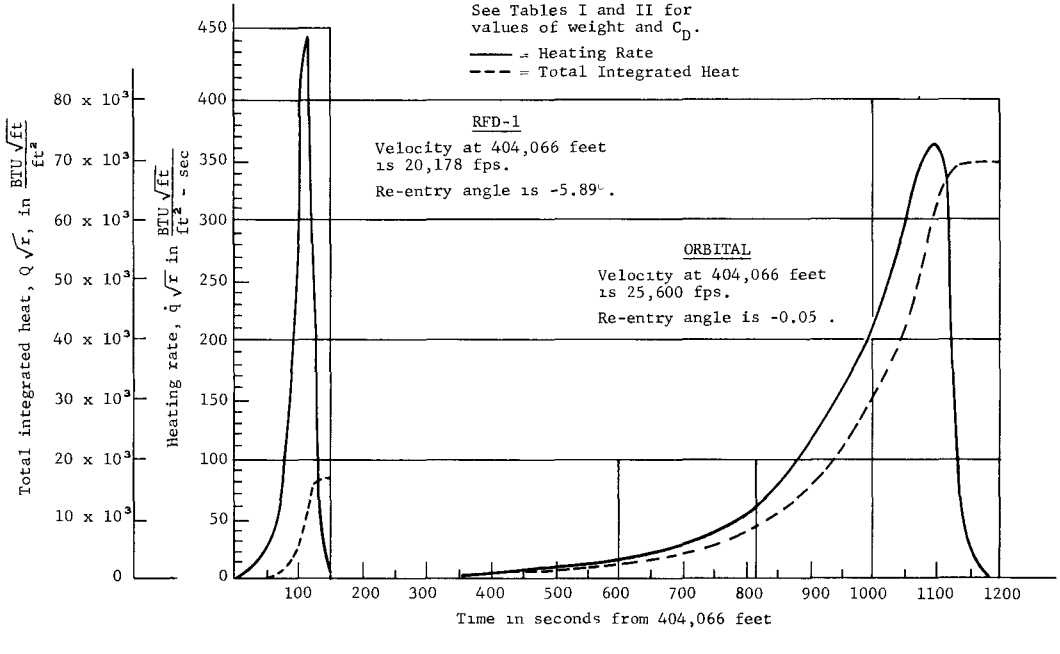


Figure 14. Comparison of heating for RFD-1 predicted re-entry and theoretical orbital decay

B. Scout Trajectory

A firm basis for the choice of the Scout as the RFD-1 launch vehicle was provided by a series of preliminary Scout trajectories (see Appendix) calculated by Chance-Vought for an assumed payload (i.e., the RS) weight and for the trajectory constraints (Section III-A) imposed on the RFD-1 flight. These trajectories indicated that the Scout vehicle could fulfill all the desired conditions except for the re-entry velocity. After the design and fabrication of the re-entry system, new trajectories were calculated, using measured RS characteristics and more refined constraints on the flight. These trajectories resulted in the determination of the pitch program for the S-116, the launch vehicle assigned to RFD-1. The RS characteristics were as follows:

| | |
|---|---|
| Weight: | 464 pounds |
| Center of gravity: | Scout Station 35.10 |
| Pitch MI: | 66.2 slug-ft$^2$ |
| Yaw MI: | 66.1 slug-ft$^2$ |
| Roll MI: | 6.12 slug-ft$^2$ |

The following constraints were included in the calculations:

1. The re-entry angle is to be -6 degrees at 400,000 feet altitude (re-entry angle is defined as the angle between the relative velocity vector and the local horizontal vector).

2. The projection of the trajectory onto the earth's surface is to be at the minimum distance from Bermuda for a flight azimuth of 129 degrees when the payload (RS) is at 150,000 feet altitude.

3. Fourth-stage motor burnout should occur at an altitude of 400,000 feet or slightly higher.

4. The vehicle longitudinal axis should be aligned with the vehicle relative velocity vector at fourth-stage motor burnout (i.e., zero degree angle of attack).

5. The Scout pitch program and stage coast periods should be optimized to provide the maximum velocity obtainable under the trajectory constraints.

Minor changes made later to the re-entry system resulted in the following final characteristics.

| | |
|---|---|
| Weight: | 482 pounds |
| Center of gravity: | Scout Station 34.89 |
| Pitch MI: | 69.6 slug ft$^2$ |
| Yaw MI: | 69.5 slug ft$^2$ |
| Roll MI: | 6.2 slug ft$^2$ |

Chance-Vought Corporation then ran a final Scout trajectory for the 482-pound RS, using the pitch program developed for the 464-pound re-entry system. Since the changes in trajectory were small, the pitch program for the 464-pound RS will be used for Scout S-116 (RFD-1). The computed conditions at fourth-stage burnout for the final Scout trajectory are:

| | |
|---|---|
| Time from launch: | 257.42 seconds |
| Altitude: | 404,066 feet above sea level |
| Range (from Wallops Island): | 323.17 nm |

| | |
|---|---|
| Latitude: | 34.292 degrees |
| Longitude: | 70.4863 degrees |
| Relative velocity: | 20,178 fps |
| Relative re-entry angle: | -5.89 degrees |
| Relative azimuth: | 132.949 degrees |
| Angle of attack: | 0.13 degree |

Figure 15 shows the calculated Scout launch vehicle trajectory for the RFD-1 flight.

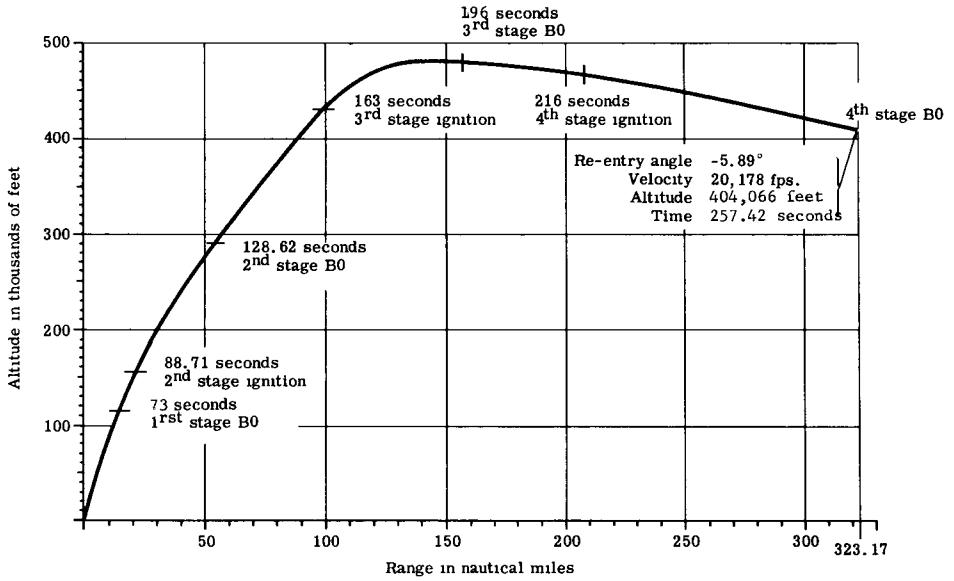


Figure 15. Nominal trajectory prediction for Scout S-116

## C. Re-entry System Trajectory

The Scout trajectory conditions at fourth-stage burnout were used as inputs to calculate the trajectory and aerodynamic heating of the re-entry system. The calculations were made using a Sandia Corporation trajectory program and the Sandia Corporation CDC 1604 computer. This program contains the complete 3-degree-of-freedom equations of motion for a point mass vehicle entering the atmosphere of a rotating oblate earth. The differential equations of motion are integrated using a modified Adams Moultan method. Although atmospheric properties can be put into the program as functions of altitude, the 1959 ARDC atmospheric model was used for all trajectories presented in this report. Previous trajectory calculations had shown that the effects of atmospheric variations on the trajectory were small.

The final re-entry system trajectory was arrived at by an iterative process. A trajectory was first run, using the estimated variation of re-entry system configuration with time (and thus the variation in drag coefficient with Mach number) and the estimated variation in re-entry system weight with altitude. The aerodynamic heating from this trajectory was then used as an input to calculate the variations in the weight and configuration of the re-entry system with time, altitude, and Mach number. Finally, the results of the computation were used to compute a new trajectory. By repeating this process until the solution converged, the final RFD-1 trajectory was obtained.

Table I gives the variation of RS weight with altitude for the final trajectory, while Table II lists the drag coefficient, $C_D$, as a function of Mach number. For the computer program, a linear variation of $C_D$ between tabulated values was assumed. The variation of drag coefficient includes the effects of changes in RS configuration resulting from reactor disassembly, as well as the variation due to Reynolds number.

TABLE I

Re-entry System Weight as a Function of Altitude

| Altitude (feet above sea level) | Re-entry System Weight (w) (pounds) | Comments |
|---|---|---|
| 400,000 to 350,000 | 482 plus burned out X-248 motor | |
| 350,000 to 242,000 | 428 | X-248 motor and external fuel rod experiment ejected at approximately 350,000 feet. |
| 242,000 to 197,000 | 405 | Reactor reflectors ejected at approximately 242,000 feet. |
| 197,000 to 75,000 | Varies from 382 at 197,000 feet to 332 at 75,000 feet | Lid of core can comes off at about 197,000 feet, followed by burning of reactor core can and RV ablation from 197,000 feet to 75,000 feet. |
| 75,000 to impact | 332 | |

TABLE II

Drag Coefficient as a Function of Mach Number
(includes effects of Reynolds number and reactor disassembly)

| Mach Number | Drag Coefficient ($C_D$) | Mach Number | Drag Coefficient ($C_D$) |
|---|---|---|---|
| 0.000 | 0.600 | 4.500 | 0.750 |
| 0.625 | 0.600 | 7.000 | 0.700 |
| 0.750 | 0.620 | 15.000 | 0.700 |
| 0.875 | 0.675 | 16.000 | 0.595 |
| 0.950 | 0.740 | 17.000 | 0.550 |
| 1.090 | 1.000 | 17.700 | 0.545 |
| 1.250 | 1.185 | 19.000 | 0.560 |
| 1.500 | 1.111 | 21.000 | 0.600 |
| 1.750 | 1.040 | 22.000 | 0.650 |
| 2.000 | 0.975 | 23.500 | 0.700 |
| 2.500 | 0.870 | 24.000 | 0.810 |
| 3.000 | 0.825 | 25.000 | 1.180 |

The drag coefficients used were based on the results of wind-tunnel tests of scale models of the re-entry system in several stages of reactor disassembly over a Mach number range of 0.5 to 22. The heating rates used to compute reactor and RV heating were based on wind-tunnel tests of aerodynamic heating of re-entry system scale models in several stages of reactor disassembly.

In computing the re-entry system trajectory subsequent to parachute deployment, the following parachute characteristics were used:

| Time (seconds after deployment) | $C_DS$ ($ft^2$) |
|---|---|
| 0 to 0.5 | Increases linearly with time from 0 to 8.6 |
| 0.5 to 10 | 8.6 |
| 10 to 10.5 | Increases linearly with time from 8.6 to 27 |
| 10.5 to impact | 27 |

The trajectories and heating rates resulting from these calculations are presented in Figures 16 through 19.

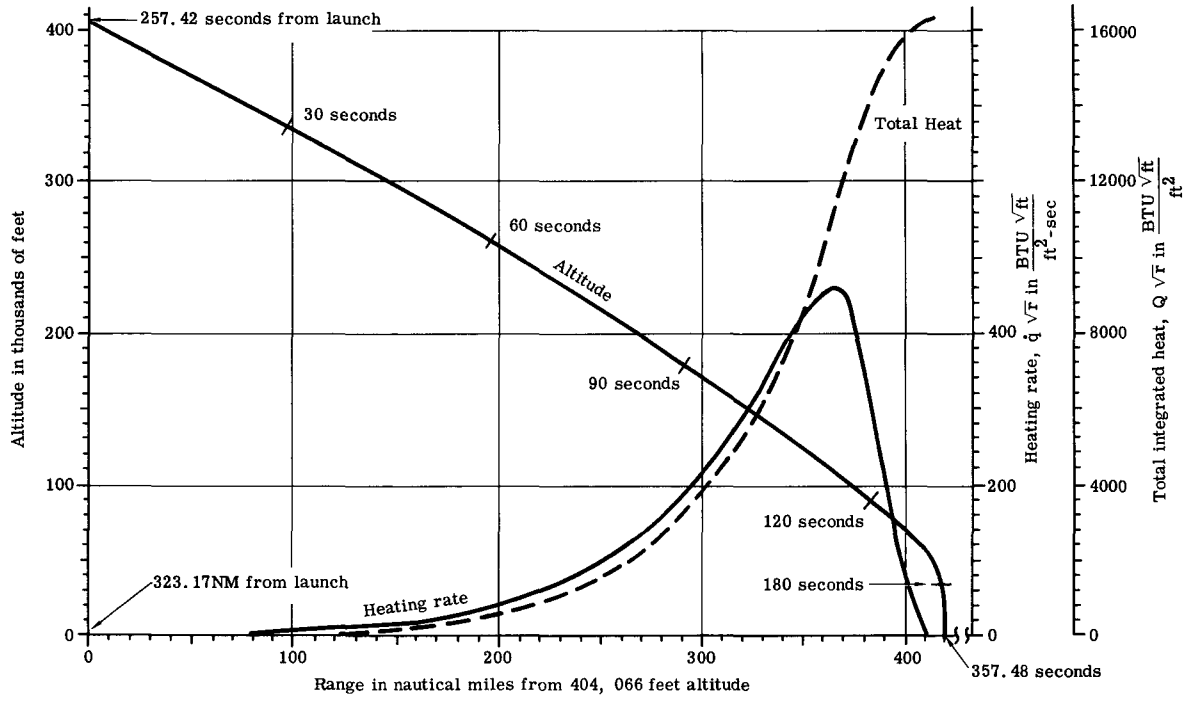


Figure 16. RS Trajectory and Heating

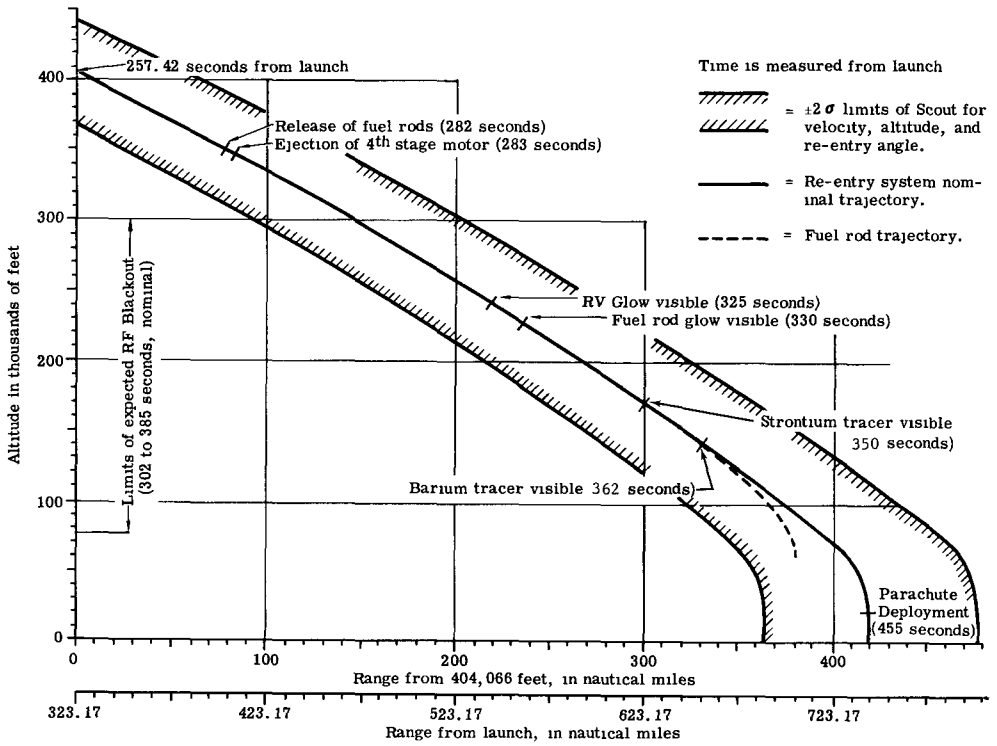


Figure 17. Re-entry event sequence as function of range

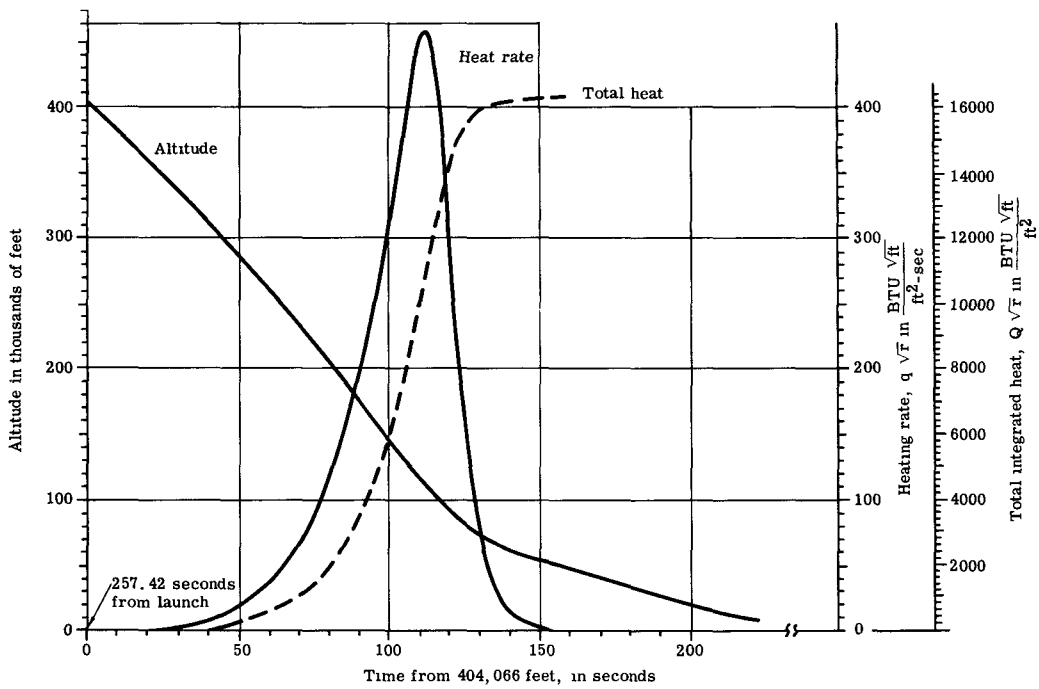


Figure 18. RS trajectory and heating as functions of time

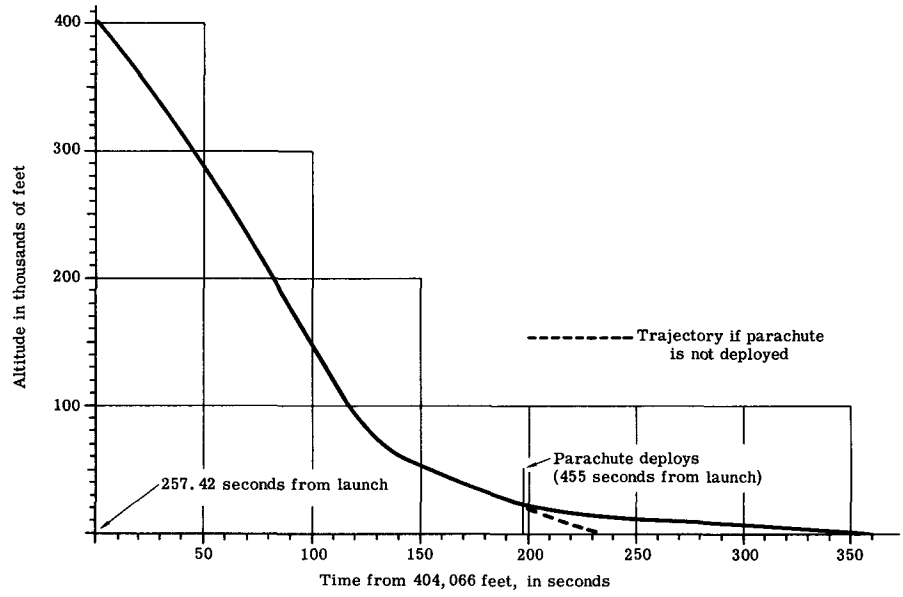


Figure 19. RS trajectory as function of time (includes parachute descent)

Variations in Re-entry System Trajectory -- The effects of variations in the Scout trajectory on the re-entry system trajectory have been determined. NASA supplied the following estimated 2-sigma tolerances on the Scout trajectory at fourth-stage burnout:

| Parameter | 2-Sigma Tolerance |
|---|---|
| Velocity | ±125 fps |
| Re-entry angle | ±0.4 degree |
| Altitude | ±36,480 feet |
| Range | ±8.2 nautical miles |
| Cross range | ±4.0 nautical miles |

The trajectory was found to be most affected by the variations in re-entry angle and altitude; therefore, trajectories were run for the following two cases:

1. Two-sigma high in altitude, two-sigma shallow in re-entry angle; and
2. Two-sigma low in altitude, two-sigma steep in re-entry angle.

These two cases, hereafter referred to as the "2-sigma pitchup" trajectory and the "2-sigma pitchdown" trajectory, are representative of the most extreme variations in the Scout trajectory that should be expected.

The trajectories for the nominal, and the 2-sigma trajectory limits are presented in Figure 17. Figure 6 (p. 13) indicates the magnitude of the effect of these 2-sigma variations on the impact point.

D. External Fuel Rod Trajectory

The initial conditions for calculating fuel rod trajectories and heating rates were obtained from the RS trajectory at the time (282 seconds) selected for ejecting the rods. Figures 20 and 21 present an average or nominal fuel rod trajectory and heating history, since individual rods may differ slightly from this because of varying ejection velocities and directions, and variations in $W/C_DA$.

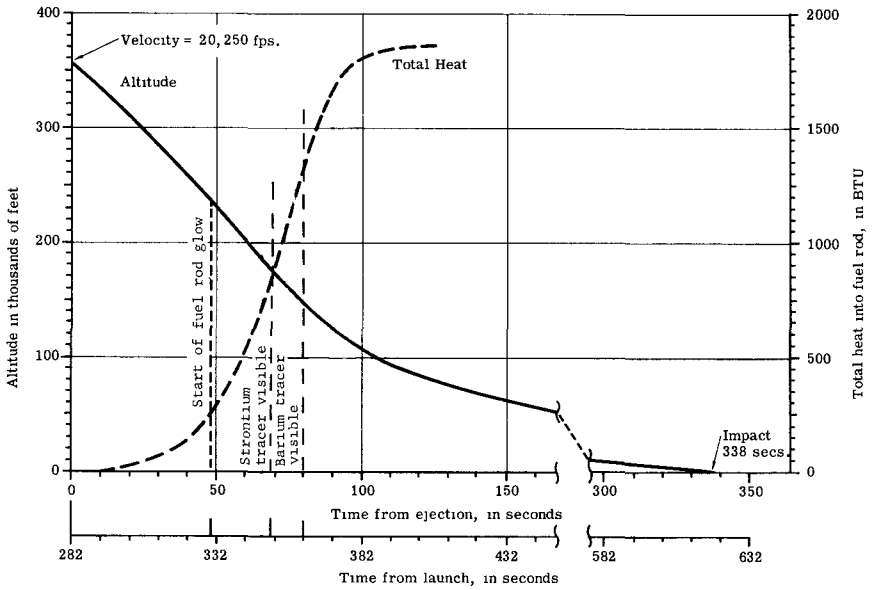


Figure 20. External fuel rod trajectory and heating

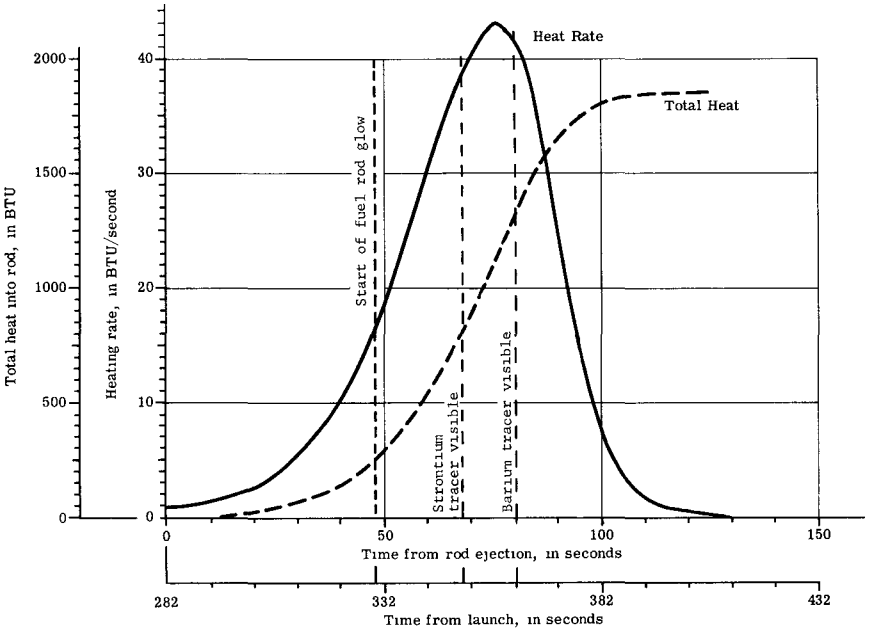


Figure 21. External fuel rod heating

E. Predicted Sequence of Events

Based on a nominal Scout trajectory, the following list presents the expected sequence of events from launch to impact. Figure 17 (p. 32) contains seven of the important re-entry events marked on the trajectory curves.

| Event | Time (seconds from launch) | Altitude (feet above sea level) |
|---|---|---|
| Ignition of 1st-stage Scout | 0 | 0 |
| Burnout and ejection of 1st stage | 73 | 117,700 |
| Ignition of 2nd stage | 89 | 155,400 |
| Burnout and ejection of 2nd stage and ejection of heat shield | 129 | 295,200 |
| Ignition of 3rd stage | 163 | 429,900 |
| Burnout of 3rd stage; firing of 4th-stage spin rockets; ejection of 3rd stage | 196 | 478,900 |
| Ignition of 4th stage | 216 | 465,300 |
| Burnout of 4th stage and start of re-entry of RV | 257 | 404,000 |
| Release of fuel rods | 282 | 357,000 |
| Ejection of 4th-stage motor | 283 | 347,000 |
| Firing of retrorockets on 4th stage motor | 286 | 340,000 |
| Blackout of TM and C-band beacon | 302-385 | 300,000-75,000 |
| Glow of RV reactor visible | 325 | 240,000 |
| Glow of fuel rods visible | 330 | 225,000 |
| Glow of ejected 4th-stage motor | 336 | 210,000 |
| Arming of parachute baroswitch | 340 | 197,000 |
| Strontium tracer visible | 350 | 170,000 |
| Barium tracer visible | 362 | 140,000 |
| Deployment of parachute | 455 | 21,000 |
| Firing (inflation) of flotation gear | 455 | 21,000 |
| Flashing light (recovery) | 455 | 21,000 |
| Energizing of SARAH beacon | 615 | 0 |

## SECTION VI -- VEHICLE AND RANGE INSTRUMENTATION

### A. Re-entry System Telemetry

Included under this heading will be the C-band radar beacon and the pyrotechnic circuitry, both of which were designed as integral parts of the telemetry proper.

1. General Description -- The telemetry for the SNAP-10A RFD-1 is composed of an FM/FM system with 10 watts of RF power of 240.2 mc/s, supplied to a "fat dipole" antenna. Eight subcarrier frequencies are used for real-time transmission of data, while three subcarriers carry information delayed 100 seconds by a tape recorder/playback system. The telemetry system is designed to provide information concerning the condition of the reactor and the RV shell; the orientation of the RS, as well as the vibration and acceleration imparted to it by the Scout; and the pressure at the head end of the fourth-stage motor.

A cone-shaped structure of Al-Mag supports the TM components and is sealed from vacuum by an aluminum cover. This entire structure is supported inside the RV by foam padding for isolation from vibration (see Figure 7, p. 17). Electrical connections to the telemetry package are provided at the rear surface of this structure. Figures 22 through 25 show the interior of the telemetry package.

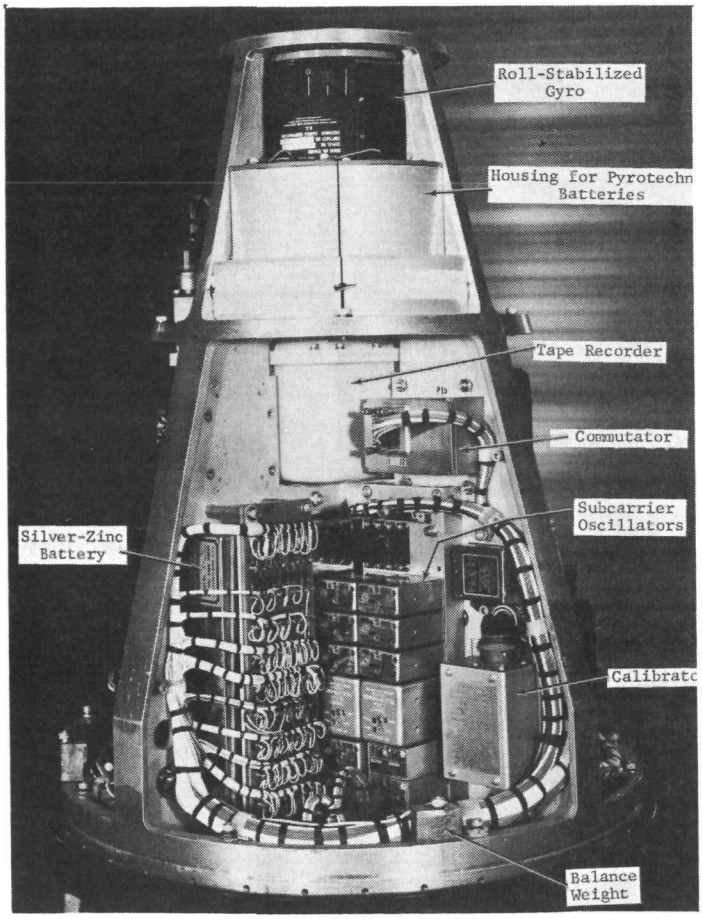


Figure 22. TM package

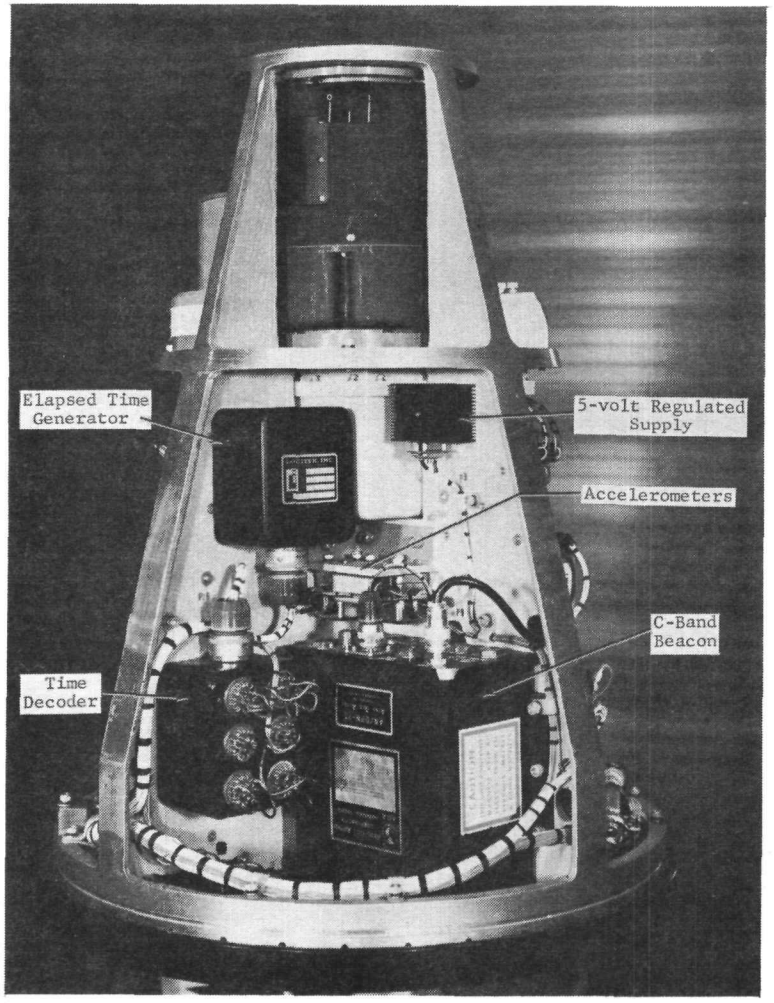


Figure 23. TM package

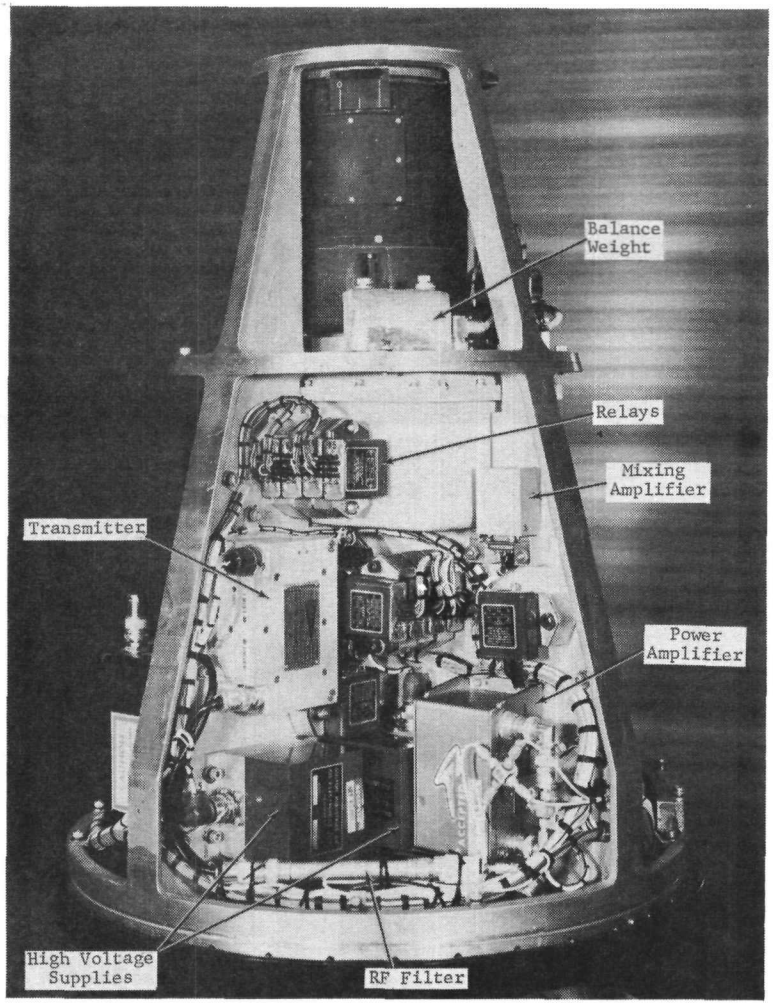


Figure 24. TM package

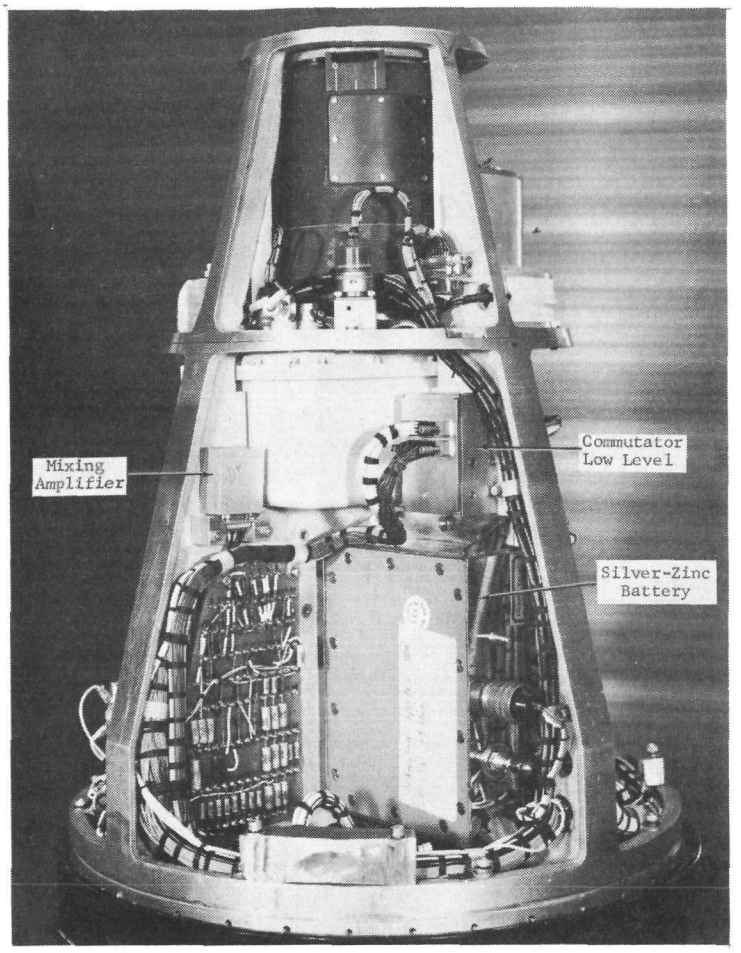


Figure 25. TM package

2. Electrical Design -- Reference to Figure 26 will aid in following the discussion below. The components used in RFD-1 are listed in Table III, while Tables IV, V, and VI show the channel and commutator allocations.

The high-level subcarriers are deviated ±7.5 percent by -1 to +5-volt signals, while the two low-level units are deviated the same percentage by a signal of -4 to -16 millivolts. Additionally, the low-level oscillators will not deviate more than +10.5 percent for input signals as high as 1.5 volts.

Vibration at the motor end of the RV adapter will be measured from launch through fourth-stage motor burning. Ejection of the fourth stage removes the signal inputs to the three vibration subcarriers, providing a signal for the telemetry to indicate that separation has occurred. These subcarriers will then be turned off by the time decoder, allowing a programmed increase in RF carrier deviation by the remaining nine oscillators.

Except for vibration, information channels are transmitted in delayed time as well as real time. In this way, data on vehicle and reactor actions during RF blackout will be transmitted during the postblackout, preimpact transmission period.

The low-level commutator carries all the temperature information: 20 reactor temperatures, 3 heat meter outputs, 3 reference junction temperatures, and one TM internal temperature. The low-level subcarrier oscillator is limited in deviation so that thermocouple outputs beyond the calibrated (16 millivolt) range can be accepted, but the oscillator cannot be deviated into an adjacent channel. This oscillator deviates linearly to at least 10 percent of center frequency.

A series of tests of the low-level thermocouple circuitry in a plasma jet indicated that no appreciable noise pickup would occur from the re-entry ion sheath. Pickup of RF from the transmitters, however, was intolerable, and it was necessary to install low-pass filters at the two low-level voltage controlled oscillators as well as to shield signal, power, and control cables entering the package.

Two platinum resistors will measure temperature in a heat-insulated junction area at the base of the reactor where all thermocouple leads are changed to copper wire leads. Another reference junction, with a nickel resistor to measure its temperature, is established in the space between the telemetry package and the RV skin to allow a similar change to copper leads for the RV thermocouple wires.

Each of the three heat meters consists of a thermocouple embedded in a known material whose heat absorption characteristic is known from previous measurements. This results in a calibration of a given number of Btu/ft$^2$ for each degree of temperature indicated by the thermocouple. Two heat meters are located on the forward cone surface of the RV, while one is placed at the base of the reactor.

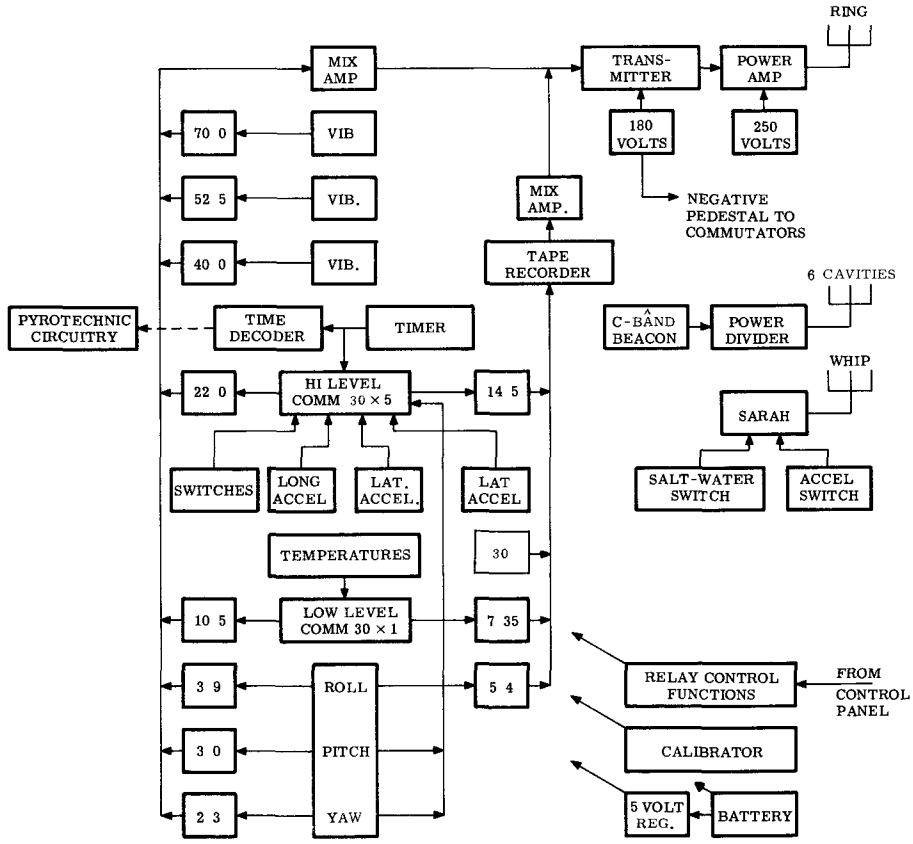


Figure 26. TM block diagram

TABLE III

RFD-1 Telemetry Components - Airborne

| | | Quantity | Manufacturer | Model or Type | Remarks |
|---|---|---|---|---|---|
| 1. | Battery, 28 volt | 1 | Eagle-Picher | MAR4096-3 | Silver-zinc |
| 2. | Power supply, 180 and -5 volt | 1 | Gulton | CG251C | Supplies pedestal to commutator |
| 3. | Power supply, 250 volt | 1 | Gulton | CG251A | |
| 4. | Regulator, +5 volt | 1 | Gulton | 280-R | |
| 5. | Oscillator, subcarrier, hi level | 10 | Teledynamics or Vector | 127-A TS-41 | |
| 6. | Oscillator, subcarrier, lo level | 2 | Teledynamics | 1284CY | Deviation limted |
| 7. | Mount, oscillator | 1 | Vector | M-137 | |
| 8. | Amplifier, mixing | 2 | Vector | TA-48 | |
| 9. | Calibrator, subcarrier | 1 | Sandia | TRC-1A | |
| 10. | Elapsed time generator | 1 | Logitek | A594-T122 | Parallel output |
| 11. | Time decoder | 1 | Logitek | A619-T149 | |
| 12. | Tape recorder/ reproducer | 1 | CEC | 178900 | To Sandia specs |
| 13. | Transmitter | 1 | Telemet | 1483A17 | 2 watts out |
| 14. | Power amplifier, RF | 1 | Teledynamics | 1114B-1 | 10 watts out |
| 15. | Gyro, roll stabilized | 1 | Whittaker Controls | 516405 | To Sandia specs |
| 16. | Commutator, hi level | 1 | Fifth Dimension | S/S3MH-342 | 30 x 5 |
| 17. | Commutator, lo level | 1 | Fifth Dimension | S/S1MH-343 | 30 x 1 |
| 18. | Accelerometer, long. | 1 | Giannini | Resistance | ±20 g |
| 19. | Accelerometer, lat. | 2 | Bourns | Resistance | ±3 g |
| 20. | Vibration system, long. | 1 | Endevco | 28130 | ±50 g |
| 21. | Vibration system, lat. | 2 | Endevco | 28130 | ±10 g |
| 22. | C-band beacon | 1 | Aero-Geo-Astro | 505 | 400-w/peak output |
| 23. | Relays, control | 14 | Leach | 9225 and 9235 | |
| 24. | Batteries, pyrotechnic | 4 | Gulton | 10V0.250 | Redundant system |
| 25. | SARAH | 1 | ACR Electronics | 4C | |

TABLE IV

RFD-1 Telemetry Channel Allocations

| SCO(kc/sec) | Measured | Magnitude | Approximate Voltage Level | Comments |
|---|---|---|---|---|
| 2.3 | Yaw | ±85° | 0 to +5 v | 3 segments/170° |
| 3.0 | Pitch | Infinite | 0 to +5 v | 8 segments/360° |
| 3.9 | Roll | Infinite | 0 to +5 v | 4 segments/360°; 180 rpm |
| 5.4 | Roll delayed | Infinite | 0 to +5 v | 4 segments/360°; 180 rpm |
| 7.35 | Commutated, temp. | 0° to 2500°F | 0 to +16 mv | Low-level delayed 100 secs |
| 10.5 | Commutated, temp. | 0° to 2500°F | 0 to +16 mv | Low-level real time |
| 14.5 | Commutated, events, accel., time | -- | 0 to +5 v | Hi-level delayed 100 secs |
| 22.0 | Commutated, events, accel., time | -- | 0 to +5 v | Hi-level real time |
| 30.00 | Recorder speed compensation | -- | -- | -- |
| 40.0 | Vibration, long. | ±50 g | ±2.5 v | Charge-amplifier system |
| 52.5 | Vibration, lat. | ±10 g | ±2.5 v | Charge-amplifier system |
| 70.0 | Vibration, lat. | ±10 g | ±2.5 v | Charge-amplifier system |

TABLE V

Telemetry
Commutated Data - 30 x 5 High Level

| Data | Magnitude | Samples per second |
|---|---|---|
| Acceleration, longitudinal | ±20 g | 10 |
| Acceleration, lateral | ±3 g | 10 |
| Acceleration, lateral | ±3 g | 10 |
| Pressure, head end X248-A6 | 0 to 400 psi | 10 |
| Elapsed time generator start | -- | 10 |
| Elapsed time | 0 to 1024 sec | 5 |
| Yaw | ±85° | 5 |
| Pitch | Infinite | 5 |
| Solar cell | Unknown | 5 |
| 28-volt monitor | 0 to +5 volts | 5 |
| Switch, ablation 1 | 0 to +5 volts | 5 |
| Switch, ablation 2 | 0 to +5 volts | 5 |
| Switch, ablation 3 | 0 to +5 volts | 5 |
| Switch, reactor A | 0 to +5 volts | 5 |
| Switch, reactor B | 0 to +5 volts | 5 |
| Switch, reactor C | 0 to +5 volts | 5 |
| Master pulse | +5 volts reference | 5 |
| Ground | 0 | 5 |

Notes: Elapsed time generator requires 5 commutator channels.
Two commutator segments are not used.

TABLE VI

Telemetry
Commutated Data - 30 x 1

| Measuring Element No. | Material | Location |
|---|---|---|
| 1 | Chromel/Alumel | Bracket, band support |
| 2 | Chromel/Alumel | Band standoff |
| 3 | Chromel/Alumel | Fin, leading (inner) |
| 4 | Chromel/Alumel | Fin, trailing (outer) |
| 5 | Chromel/Alumel | Fin, leading (inner) opposite No. 3 |
| 6 | Chromel/Alumel | Fin, trailing (inner) |
| 7 | Chromel/Alumel | Bandjoint |
| 8 | Chromel/Alumel | Bandjoint 180 degrees away |
| 9 | Pt/Pt-13% Rh | NaK tube, transverse, leading surface |
| 10 | Pt/Pt-13% Rh | NaK tube, transverse, trailing surface |
| 11 | Pt/Pt-13% Rh | Base of NaK pump |
| 12 | Pt/Pt-13% Rh | NaK fill tube |
| 13 | Pt/Pt-13% Rh | Lip weld, behind NaK tube |
| 14 | Pt/Pt-13% Rh | Lip weld in open |
| 15 | Pt/Pt-13% Rh | Lip weld behind fin |
| 16 | Pt/Pt-13% Rh | Lip weld, behind NaK tube, opposite No. 13 |
| 17 | Pt/Pt-13% Rh | Lip weld in open, opposite No. 14 |
| 18 | Pt/Pt-13% Rh | Lip weld behind fin, opposite No. 15 |
| 19 | Pt/Pt-13% Rh | Core vessel wall |
| 20 | Pt/Pt-13% Rh | Core vessel wall, opposite No. 19 |
| 21 | Chromel/Alumel | Base of reactor - Sandia heat meter |
| 22 | Pt. resistor | Reactor reference junction |
| 23 | Pt. resistor | Reactor reference junction |
| 24 | Chromel/Alumel | RV nose, front, heat meter |
| 25 | Chromel/Alumel | RV nose, rear, heat meter |
| 26 | Nickel resistor | RV reference junction |
| 27 | Thermistor | TM package |

Internal telemeter temperature is monitored by means of a thermistor placed on the support structure near the power amplifier.

At the head end of the X-248 motor, NASA will install a pressure transducer whose output will be sampled by the high-level commutator 10 times every second.

The elapsed time generator (or timer) supplies time-of-fire signals to the time decoder for the pyrotechnic circuitry and is sampled by the high-level commutator to supply a time reference for the airborne tape.

The timer output consists of 10 parallel, binary-coded pulses which provide time information, in 1-second increments, up to 1048 seconds. These 10 signals comprise the inputs to the time decoder. They are also multiplexed onto five segments of the high-level commutator and transmitted in real and delayed time.

The calibrator provides three voltages of known value to the inputs of all high-level oscillators. This calibration will be last performed just before launch. Low-level oscillators are not calibrated since the commutated signal contains +16 millivolts and ground as reference levels.

3. Mechanical Design -- The shape of, and volume allotted to, the TM package was determined by the design of the RV. Because of the magnitude of vibration expected from the X-248 motor, the TM structure was designed to be cradled in a polyurethane foam bed. The result was no metal-to-metal contact between the TM package and the RV (see Figures 7 and 8, pp. 17 and 19).

The TM structure, as designed, successfully passed the qualification tests as an integral unit of the RS. Fabricated in the same manner, the two flight-test structures survived the acceptance testing of the RS with no difficulties.

4. Antenna Design -- The TM antenna for RFD-1 is basically a dipole type in which the wires constituting the dipole are replaced by large-diameter, hollow cylinders. Like the ordinary dipole, this antenna is fed across the gap between the two halves. To attain as closely as possible the desired pattern and polarization, and to minimize the possibility of breakdown across the gap, this antenna is fed at three equally spaced points around the circumference at the gap. The coordinate system used and the antenna pattern are shown in Figures 27 and 28.

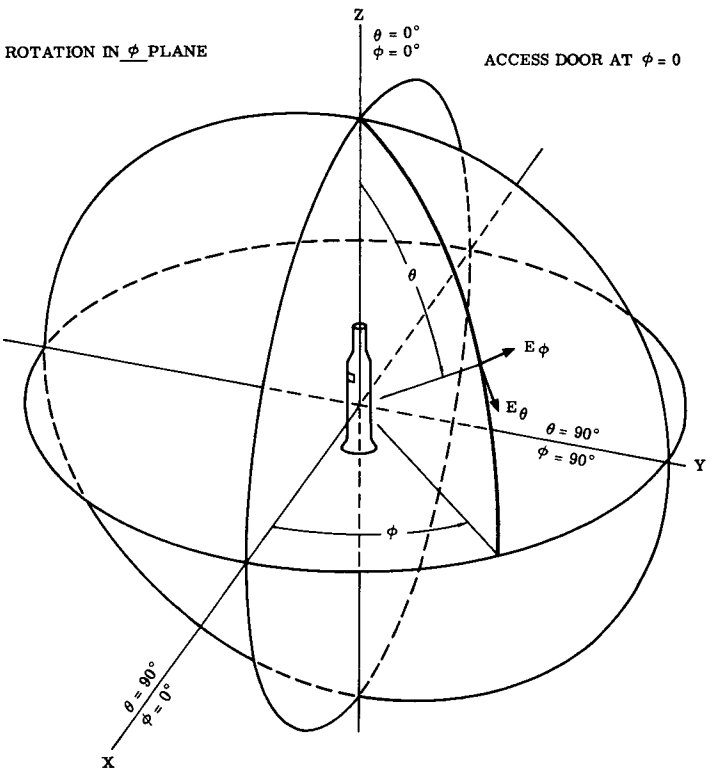


Figure 27. Antenna pattern coordinate system (telemetry)

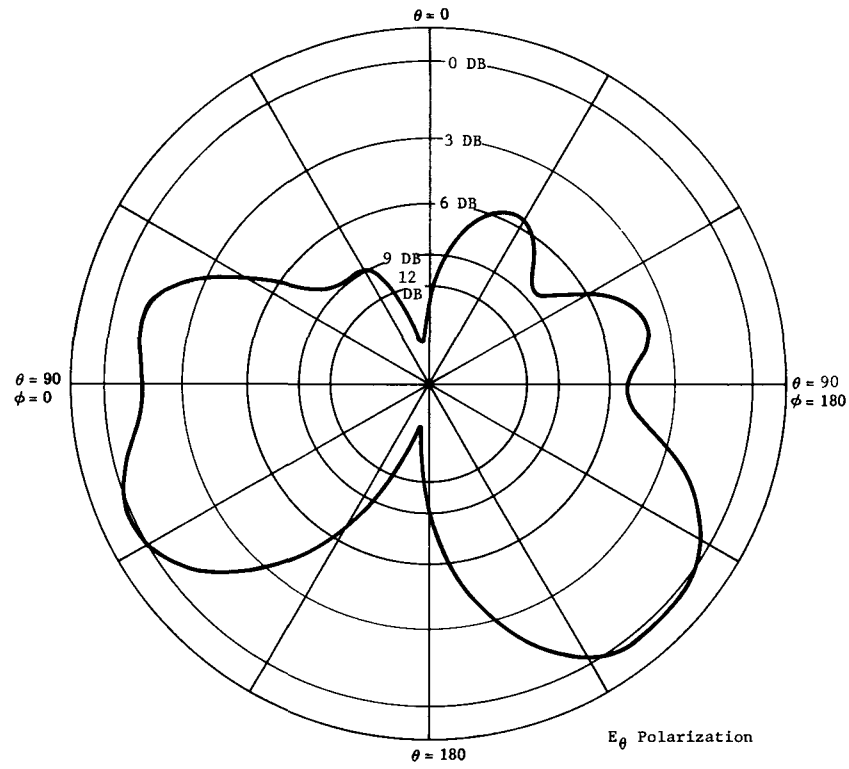


Figure 28. TM antenna pattern

Testing of the antenna system in a high vacuum with full RF power, showed that no breakdown problems were present.

The antenna consists of two aluminum cylinders, each 11 inches long, separated by a gap of 0.4 inch, placed within the body of the RV as shown in Figure 10, p. 21.

5. C-Band Beacon System -- Since it is important that the re-entry trajectory of RFD-1 be accurately known, the FPS-16 radar at Bermuda will track the RS during this portion of the flight. To assure an adequate return signal to the FPS-16, a radar transponder is included in the telemetry package. This transponder, or beacon, supplies 400 watts of RF power, when triggered by the interrogating ground radar, to a set of six cavity antennas located on the forward cone of the RV shell. A power divider is used for impedance transformation to properly load the beacon and assure each cavity of an equal amount of power. The cavities are designed to radiate the signal as far forward of the vehicle as possible, given the limitations of the vehicle design and the required placement of the antenna. As was stated before, the cavities are covered with Teflon which, in contrast to phenolic fiberglass, is transparent to RF during ablation. Testing in a vacuum chamber indicated that no arc-over or breakdown would occur under the full power output of the beacon at the maximum altitude expected during the flight. The coordinate system used and the antenna pattern are shown in Figures 29 and 30.

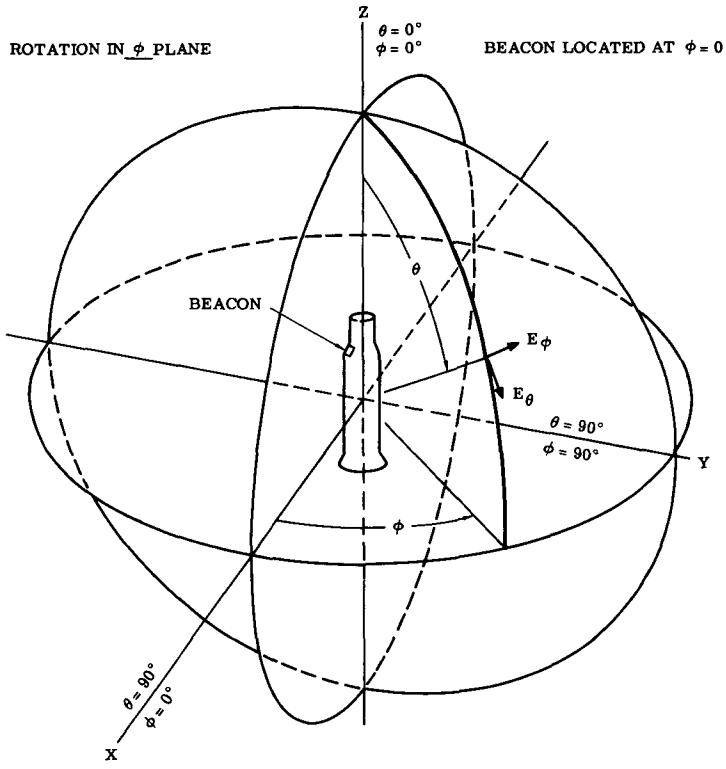


Figure 29.

Antenna pattern coordinate system (beacon)

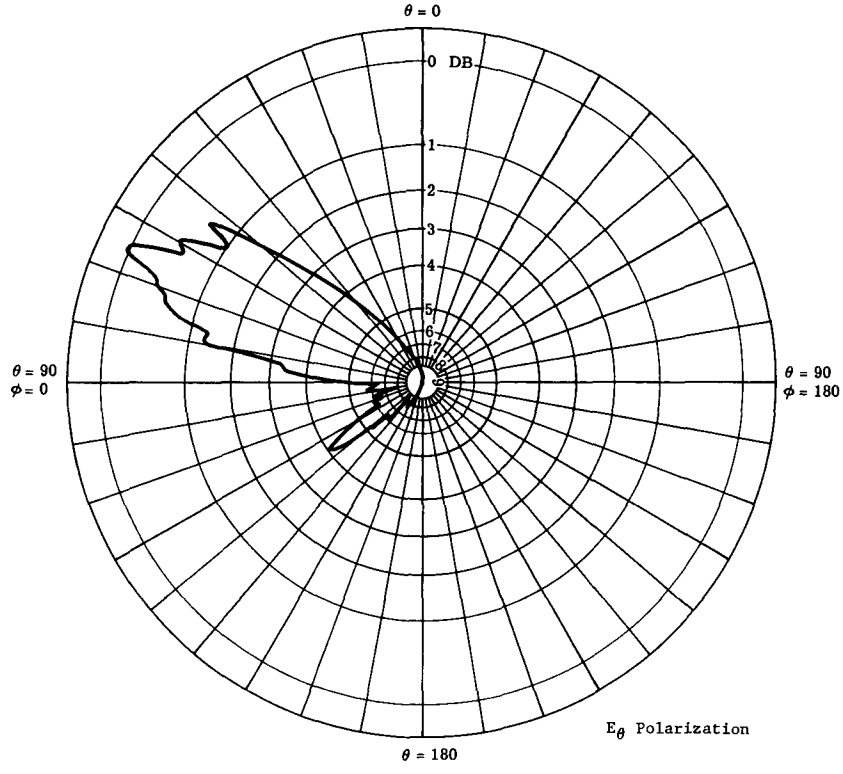


Figure 30.

C-band antenna pattern

6. Pyrotechnic Circuitry -- The batteries and relays for firing the pyrotechnic squibs are packaged as a part of the telemeter structure. (See Figure 31 for the block diagram.)

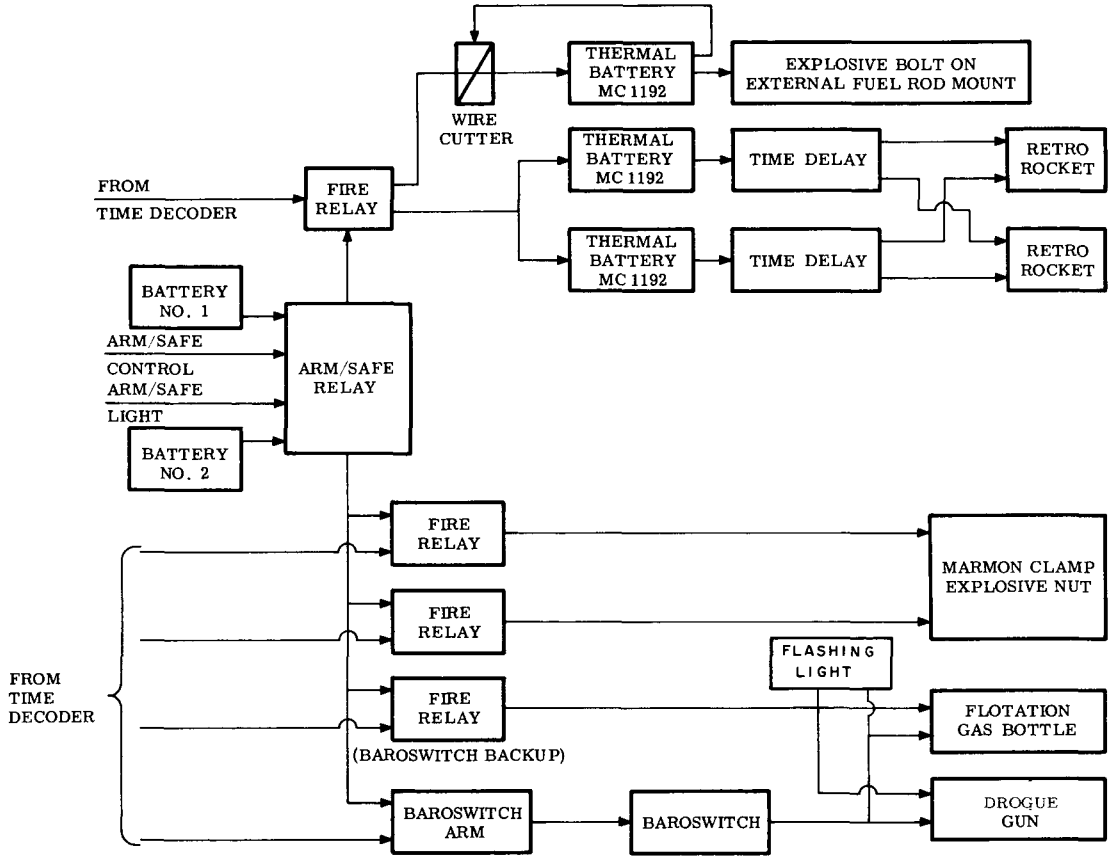


Figure 31. Block diagram of pyrotechnic circuitry

As mentioned above, the outputs from the elapsed time generator are supplied to the time decoder, which provides signals for relay closures at the desired preselected times. As a precaution, to prevent excessive battery drain if any squib does not change to a high resistance after firing, the time decoder is designed to hold the fire relay closed for only 1 second. Arming and safing of the squib fire circuitry will be controlled from the blockhouse by a switch on the TM control console.

To delay the firing of the retrorockets on the fourth stage until after that stage has been ejected from the RV, two electronic time delay relays are employed. The main squib batteries in the telemeter package fire two thermal batteries, and these in turn power the delay relays and fire the retrorocket squibs.

The primary fire control for the parachute and flashing light is a baroswitch which is armed by the time decoder after the RV has risen above the operate altitude setting for the device; however, if the baroswitch has not operated by the time corresponding to the preset altitude, the time decoder will provide a signal to operate the parachute and light.

B. SARAH

The SARAH (Search and Recovery and Homing) beacon is wired to be turned on either by an acceleration switch at water impact or by a Sandia-designed salt-water switch. The SARAH operates on a frequency of 235 mc/s, with a power output of 25 watts, which is fed to a Sandia-designed whip and ground-plane antenna located at the aft end of the RV.

C. Flashing Light Beacon

This device is a recovery aid which emits very short light pulses approximately once per second. It is located in the flare at the aft end of the RV and will be energized at parachute deployment to provide flashes of one-half million peak lumens for visual location of the falling RS.

D. Range Instrumentation

1. Wallops Island -- (For prelaunch checkout of RFD-1.) A small ground station will be installed in the Scout blockhouse. This will permit monitoring both the TM and the C-band beacon during the preflight checkouts and during the countdown.

All the facilities and capabilities of the Island, described in Section IV-H, will be employed during the flight.

2. Bermuda -- The NASA Mercury station at Bermuda will provide radar and telemetry coverage for RFD-1. To provide the required optical coverage for this flight, Sandia has installed, tested, and will operate the following equipment at High Point:

a. ME-16 Tracking Mount

(1) 120 inches, f.l., 70-mm, Photo-Sonics 10B, 90 fps

(2) 18 inches, f.l., Paxar, 35-mm Mitchell, 96 fps

(3) 2 inches, f.l., 35-mm Mitchell, 96 fps

b. LA-24 Tracking Mount

(1) Streak spectrograph on 120-inch main tube

(2) Sampling photometer

(3) 40 inches, f.l., 35-mm, Mitchell, 96 fps

c. Plate Cameras

(1) Three each using 12 inches, f.l. and f2.5 lenses and 10 x 12-inch glass plates

d. Plate Spectrographs

(1) Six each, using 12 inches, f.l. and F2.5 lenses, 10 x 12-inch glass plates, and B&L 600 lines/mm transmission gratings

e. Plate Trajectory Cameras

(1) Three each, K-37 cameras, 12 inches, f.l. and f2.5 lenses modified to use 12 x 12-inch glass plates

f. Cinespectrograph

(1) One each, 70-mm, Photo-Sonics 10A, 4 inches, f.1. and f2.0 lenses and B&L 600 lines/mm transmission grating, hand tracked, and operated at 10 fps

g. Hand-Tracked 16-mm Camera

(1) Six-inch f.1. and f2.5 lenses, 16-mm Bell & Howell, 126 fps

3. Aircraft -- Sandia has installed and will operate telemetry, optical, and SARAH receiving equipment aboard two AFSWC C-54 aircraft. Each TM station consists of two antennas, four receivers, a diversity combiner, and a magnetic tape recorder. The optical equipment is composed of one Streak spectrograph with an F2.5, 12-inch focal length lens, and a 16-mm Milliken motion picture camera, with a 6-inch focal length, f2.5 lens, operating at 400 frames per second. In addition, one aircraft will have a sampling photometer on board.

To supplement the Sandia airborne stations, AMR will provide at least one, and perhaps two, J130 aircraft equipped to receive and record the telemetry signal as well as the SARAH beacon. Two P5M aircraft from Bermuda will be furnished by Naval Air Station and will be used as primary search aircraft, being equipped only to receive the SARAH beacon.

4. Ships -- ORV-Gulf and NASA Range Recoverer will have TM station and SARAH receiving capability.

The minesweeper is to assist in the recovery operation and has no instrumentation equipment on board.

## SECTION VII -- GROUND TESTS

### A. Qualification Tests

Two complete test vehicles, in flight-ready condition, were subjected to the following tests:

1. Temperature Cycling --

a. RS Without TM Package -- The re-entry system with the telemetry package removed was subjected to two cycles as shown in Figure 32. Thermal stresses expected during re-entry were simulated at the RV surface to test for thermal stresses in the ablation material.

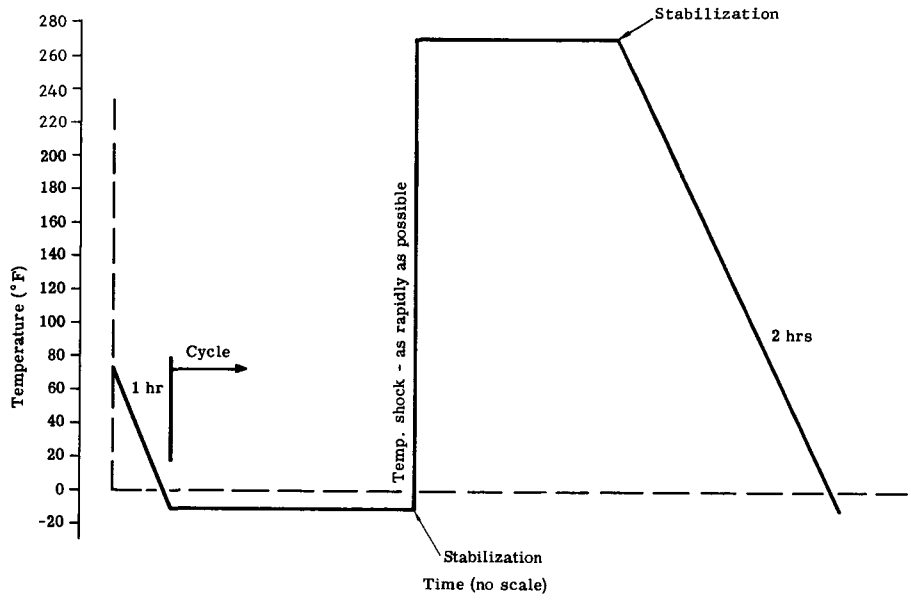


Figure 32. Temperature cycling test, RS without TM package

Relative motion of the Teflon antenna windows and the fiberglass-phenolic case cannot be accomplished by thermal shock without actually ablating the surface at a rate similar to re-entry. However, this motion was simulated by increasing the temperature gradually to a point where differences in the coefficients of thermal expansion gave the desired relative motion to test the RTV-cohrlastic bond. The RS was instrumented with strain gages and thermocouples for this test.

b. RS With TM Package -- The temperature-cycling test of the entire RS simulated temperature extremes expected during storage, transportation, and at the launch site. The temperature cycle for this test, shown in Figure 33, was not as severe as the cycle for test (a). The telemetry system was operated periodically during the two cycles of this test.

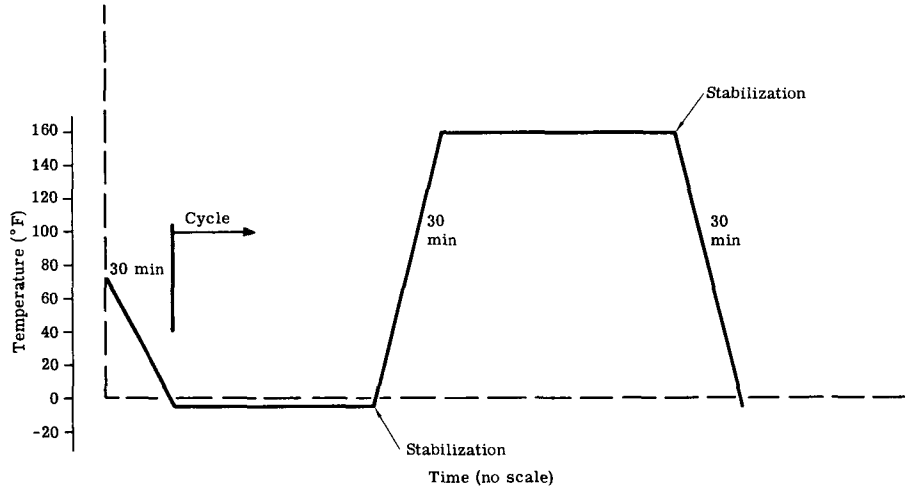


Figure 33. Temperature cycling test, RS with TM package

2. Sine Vibration -- The test vehicle was mounted on the fabricated vibration fixture which was machined to simulate the Scout fourth-stage rocket mounting configuration. After the vibration table had been equalized with a simulated rigid weight, the test vehicle was subjected to a constant-force sine sweep test along its thrust axis only. The input force was held constant at 500 pounds, and the frequency was swept from 10-2000-10 cps at a rate of two octaves/minute. The on-board telemetry was functioning during the tests.

3. Random Vibration -- The sine vibration fixture was used also for the random vibration test. For the random vibration test, the vibration table was equalized, with the test vehicle mounted to the fixture. The test vehicle was then subjected to a random vibration test along its thrust axis only, with approximately 500-rms pounds force input over-all in the frequency band of 20-2000 cps for 4 minutes. The on-board telemetry operated during the test.

4. Linear Acceleration -- The test vehicle was subjected to linear acceleration as follows: 18.75-degree tilt, 16.5 g - 3 minutes; 36.8-degree tilt, 11.25 g - 3 minutes. The tilt angle was measured between the vehicle longitudinal axis and the direction of the acceleration. The on-board telemetry was operated before and after each test.

5. Shock -- The complete test vehicle was subjected to three, 30-g peak, one-half sine-shaped, 15-msecs duration shocks along the thrust axis in the direction of thrust. The on-board telemetry was operated during the test.

6. Radiant Heat -- The purpose of these tests was to determine heat paths and temperature distributions throughout the RS during and after re-entry. Ablation of the surface took place during these tests; however, because of the absence of flow and the presence of oxygen, ablation characteristics were different from what they will be under actual re-entry conditions. The heating profiles used in the tests are shown in Figures 34 through 37.

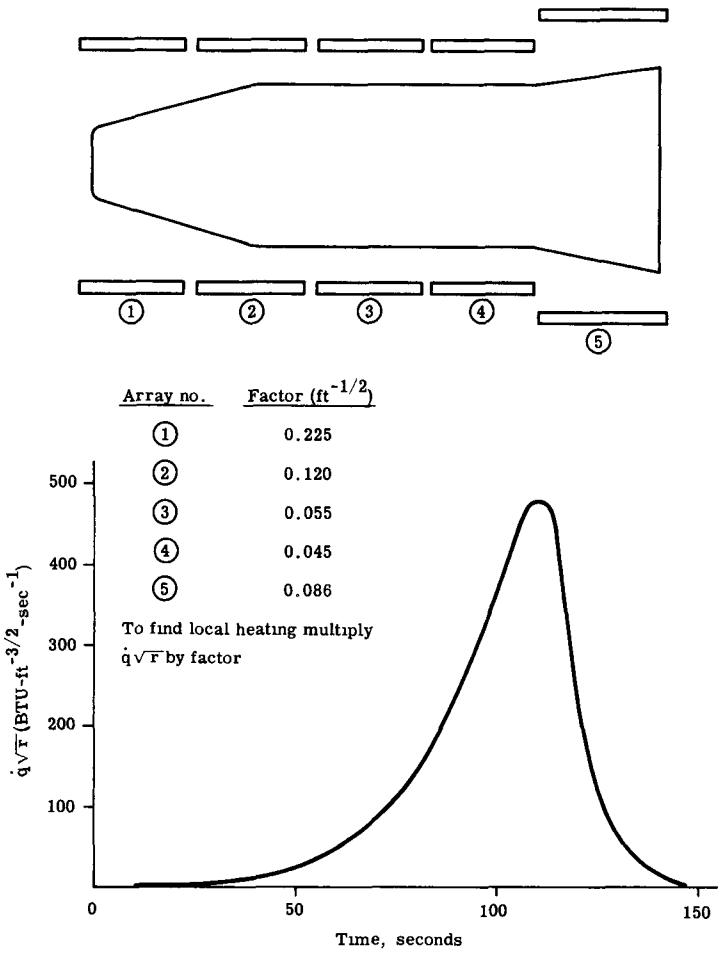


Figure 34. Requested radiant heat inputs for first full scale unit

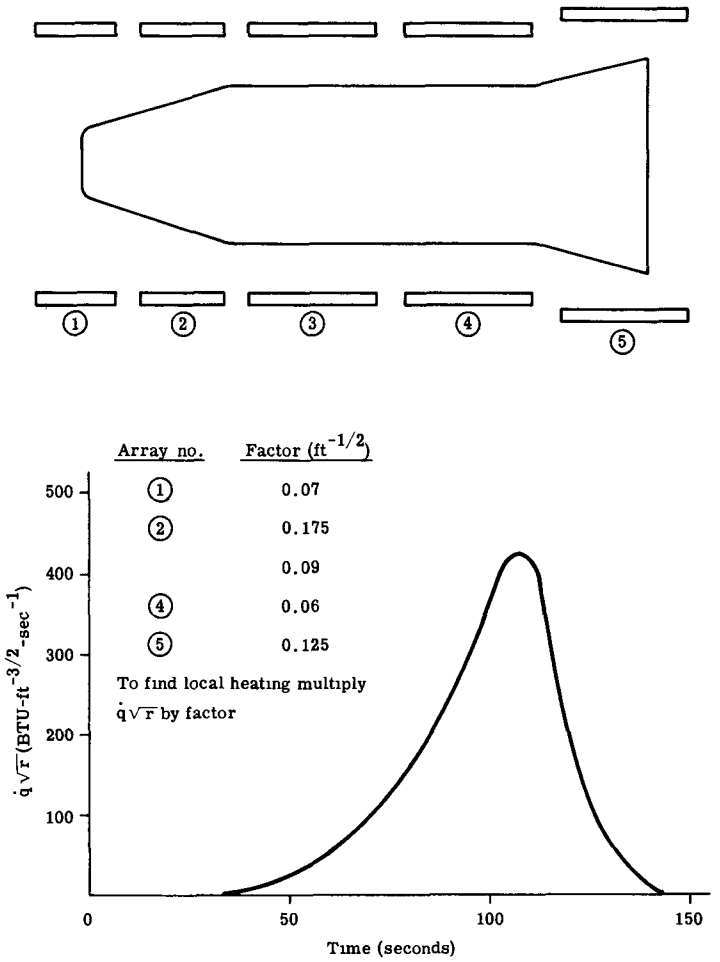


Figure 35. Requested radiant heat input for second full scale unit

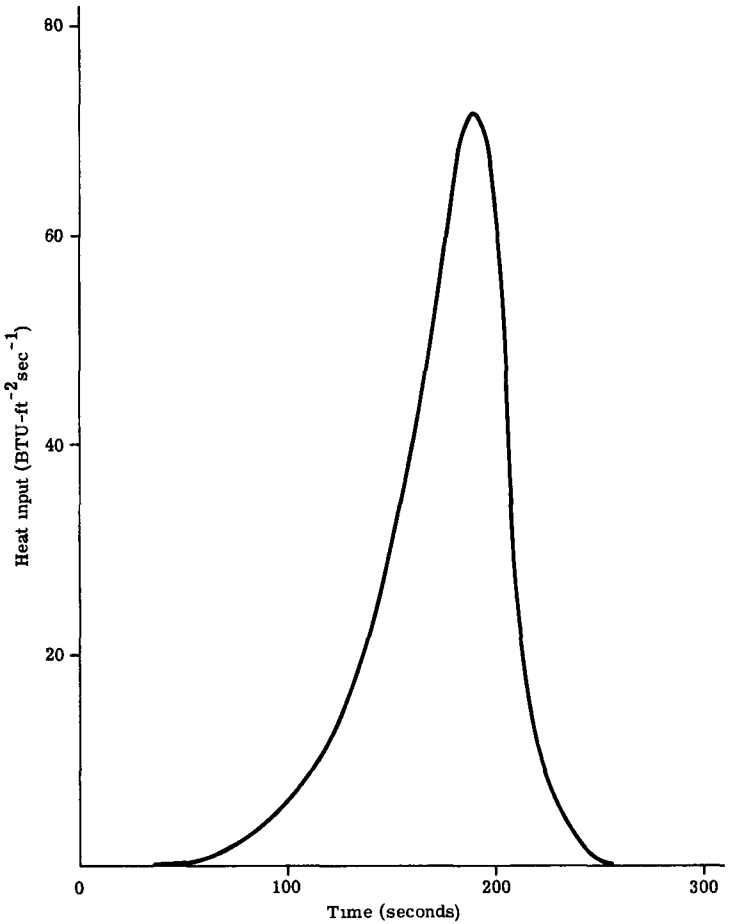


Figure 36. Radiant heat input for nose cone test

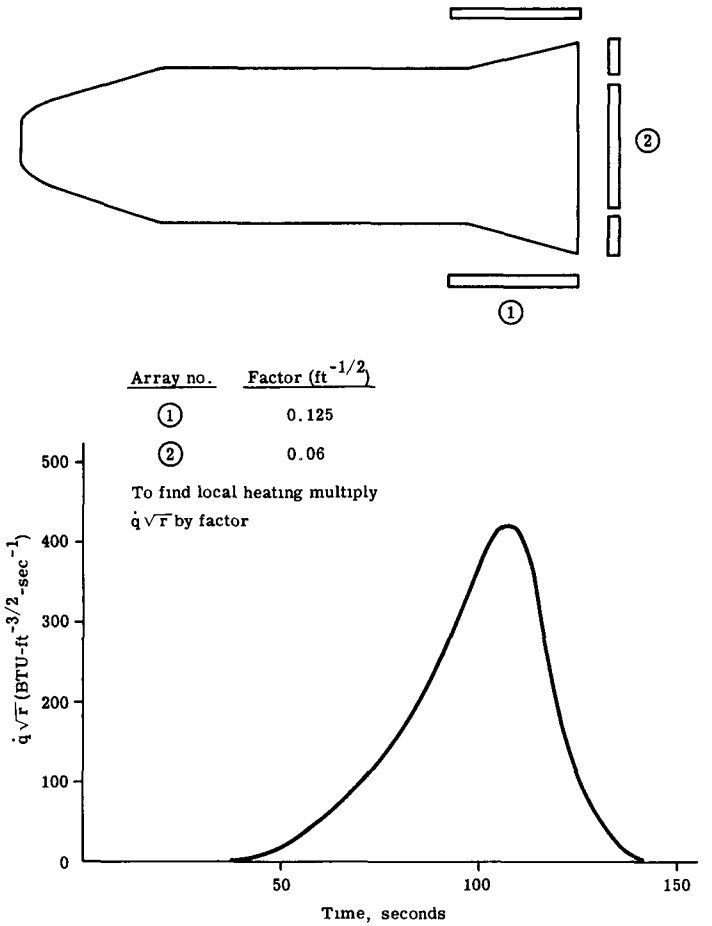


Figure 37. Requested radiant heat input for flare

7. Acoustical Noise -- The complete test vehicle was subjected to the following acoustical noise for 4 minutes:

| Octave Band | Sound Pressure Level |
|---|---|
| 20-75 | 138.5 db* |
| 75-150 | 142.5 |
| 150-300 | 141.2 |
| 300-600 | 139.6 |
| 600-1200 | 138.5 |
| 1200-2400 | 138.8 |
| 2400-4800 | 136.3 |
| 4800-9600 | 135.6 |

Over-all SPL is 148.5 db

*Ref. 0.0002 dyne/cm$^2$.

The on-board telemetry was operated during the test.

8. Spin and Spin-Balance -- The complete test vehicle was dynamically balanced while spinning about its longitudinal axis at 165 rpm. It was balanced to within 200 oz-in$^2$.

The complete test vehicle was mounted on a spin table and spun for 3 minutes about its longitudinal axis at a rate of 180 rpm. The on-board telemetry was operated before, during, and after each test.

9. Hypersonic Wind Tunnel -- Tests on full- and quarter-scale models were run in the AEDC, 100-inch, hot-shot tunnel to determine ratios of local-to-stagnation heating rates. These ratios were obtained by means of heat meters on the cone, cylinder, and flare of the RV and at numerous locations on the reactor. Ratios for the RV were obtained with the reactor but without reflectors, while reactor ratios were obtained with and without the NaK pump.

Heat distribution along the reactor and RV was found to be a function of Reynolds number and configuration. Ranges at specific locations are as follows:

| Location | $\dot{q}$ local/($\dot{q}$ stag $\sqrt{R}$) |
|---|---|
| NaK fill tube | 3.4 |
| Forward NaK tube | 2.2 - 4.2 |
| Leading edge of fin | 5.0 |
| Side of fin | 0.090 - 0.115 |
| Leading side of pump | 1.5 - 2.3 |
| Front of can (without pump) | 0.9 - 2.3 |
| Front of can behind pump | 0.35 |
| Front of can outboard of pump | 2.2 - 3.1 |
| Can lip behind NaK tube | 0.15 - 0.40 |
| Can lip in open | 3.2 |
| Can lip behind fin | 0.4 - 0.7 |
| Can lip (without pump) | 1.1 - 2.5 |
| Upper side of can | 0.07 - 0.16 |

| Location | $\dot{q}$ local/($\dot{q}$ stag $\sqrt{R}$) |
|---|---|
| Lower side of can | 0.02 - 0.15 |
| Leading edge of can base | 0.7 - 1.3 |
| Side edge of can base | 0.07 - 0.18 |
| Separated region behind reactor | 0.005 - 0.020 |
| Fore cone RV | 0.11 - 0.20 |
| Aft cone RV | 0.07 - 0.13 |
| Fore cylinder RV | 0.03 - 0.10 |
| Aft cylinder RV | 0.015 - 0.045 |
| Fore flare RV | 0.04 - 0.11 |
| Aft flare RV | 0.05 - 0.130 |
| Attached fuel rod experiment | 2.25 |

B. Acceptance Tests

The weight, CG, and MI of each of the two complete test vehicles, in flight-ready condition, were determined. Further, each complete test vehicle, in flight-ready condition, was subjected to the following tests:

1. Sine Vibration -- The test vehicle was mounted on the fabricated fixture which had been machined to simulate the Scout fourth-stage rocket mounting configuration (Section VII-A2). After the vibration table had been equalized with a simulated rigid weight, the test vehicle was subjected to a constant-force sine sweep test along its thrust axis only. The input force was held constant at 350 pounds, and the frequency was swept from 10-2000-10 cps at a rate of two octaves per minute. The on-board telemetry was operated before, during, and after the tests.

2. Random Vibration -- Using the same vibration fixture that was used for the sine vibration test, the vibration table was equalized, with the test vehicle mounted to the fixture. The test vehicle was then subjected to a random vibration test along its thrust axis only, with a 350-rms force input over-all in the frequency band of 20-2000 cps for 4 minutes. The on-board telemetry was operated before, during, and after the test.

3. Temperature Cycling -- Each SNAP-10A re-entry system to be launched was subjected to two cycles of the test defined in Section VII-A1b, with the telemetry operating.

4. Spin and Spin-Balance -- The complete test vehicle was dynamically balanced while spinning about its longitudinal axis at 165 rpm. It was balanced to within 200 oz-in$^2$.

The complete test vehicle was mounted on a spin table and rotated for 3 minutes at 180 rpm about its longitudinal axis. The on-board telemetry was operated before, during, and after each test.

## SECTION VIII -- SCHEDULE

The RFD-1 test schedule is shown in Figure 38.

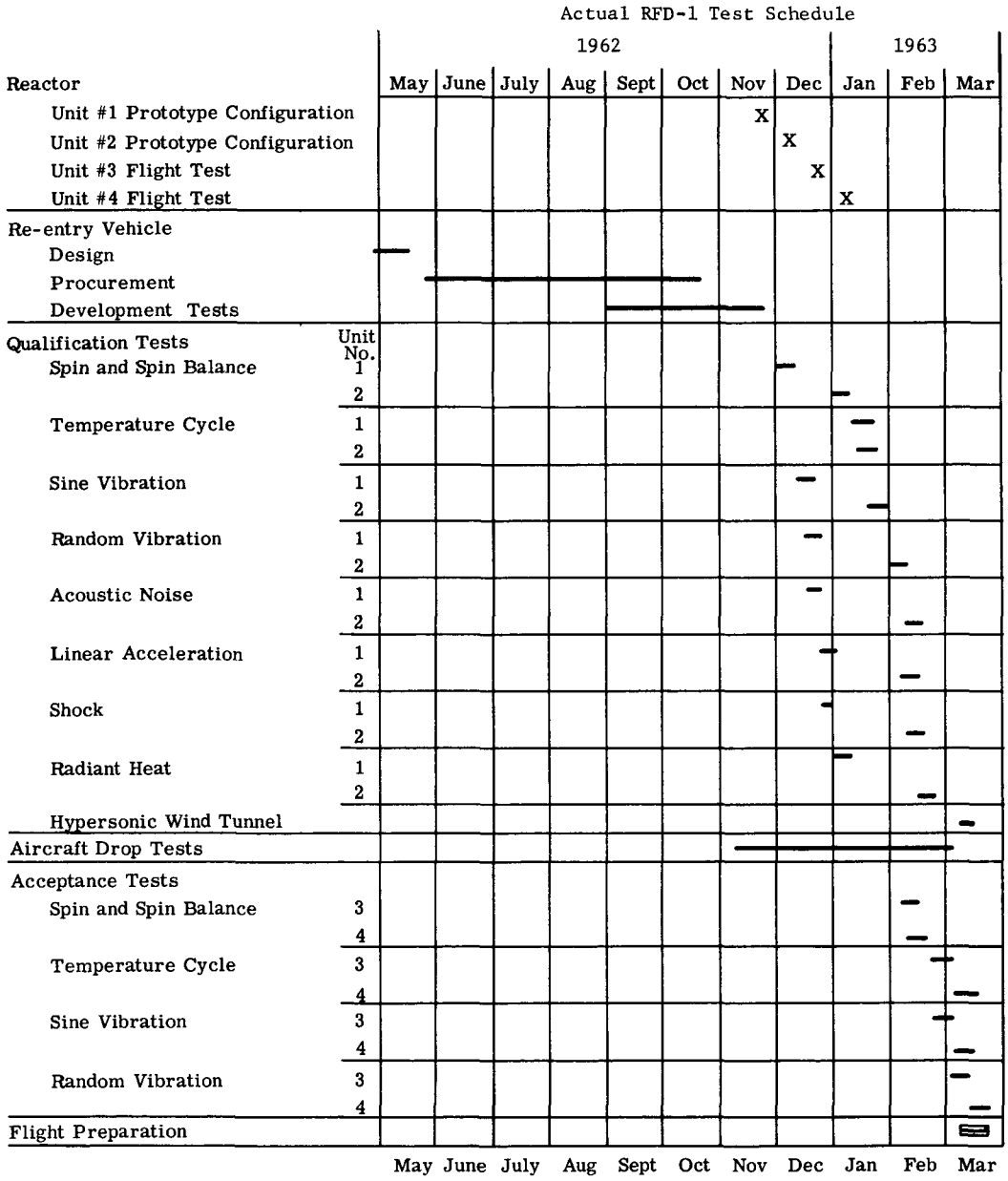


Figure 38. RFD-1 Test Schedule

## SECTION IX -- ORGANIZATION RESPONSIBILITIES - JWG

The Joint Working Group (JWG) for the SNAP-10A (inert) re-entry flight demonstration to be known as "RFD-1" is organized to define in detail the responsibilities of each of the supporting agencies of the flight-test program. It will, in addition, define the timetable of events to meet the objectives of the flight-test program through launch and recovery. The organization of the RFD-1 JWG is as follows:

| Agency | Responsibility | Representative | First Alternate |
|---|---|---|---|
| Sandia Corporation* | Mission Director | A. E. Bentz | A. J. Clark |
| NASA Wallops Station | Test Director | Larry Early | Steve Diamond |
| NASA Scout Project Office | Payload Coordinator | Allen Churgin | Bob Schmitz |
| Chance Vought Astronautics | Scout Vehicle Contractor | Kenneth Jacobs | Sam Lynne |
| Atomics International | Reactor Manufacturer | Robert Detterman | Roger Elliot |
| AEC/Div. Reactor Dev. | Program Director | Lt. Col. Werner Kern | Charles McCallum |
| AFSC/AFSWC | Aircraft Support | Maj. Baker | Maj. P. McMullen |
| AFSC/AFMTC | Sea Support | | |

*Denotes Chairman, Joint Working Group.

## SECTION X -- WALLOPS RANGE DESCRIPTION

### A. General

Wallops Station, which is a facility of the National Aeronautics and Space Administration, is located on the Atlantic Coast of the Delmarva Peninsula. The station was established in 1945 to obtain aerodynamic data of transonic and low supersonic speeds.

### B. Definition

As a member of the NASA organization, Wallops Station is part of the Office of Space Flight Programs and is under direct cognizance of the Director of that office. Wallops Station can be defined as a small but flexible space-flight station designed to handle and test vehicles from the smallest up to types (such as the Scout) with orbital capabilities.

### C. Purpose

The present-day function of Wallops Station is to conduct experiments with rocket-propelled vehicles carrying payloads for aeronautical and space research. These payloads may be in the form of re-entry or space flight models, models of manned space capsules, ionized layer data-gathering and other sounding devices, or any other space research device capable of being carried by the vehicles which Wallops Station can launch. Facilities are available at Wallops Station to gather research data from such vehicles. In addition to radar and telemetry, most tests are supported at Wallops Station with photographic coverage and optical tracking facilities.

### D. Range Capability

Wallops Station maintains an instrumented test range consisting of integrated mainland and island facilities for conducting tests using rocket-propelled test vehicles. All such vehicles launched at Wallops Station utilize the Atlantic Ocean as the test range. The actual range area, as defined by azimuth and elevation for a given test, is limited at Wallops Station only by safety considerations. Since the rocket vehicles used to conduct the majority of tests are proven types, performance data are available to facilitate predictions of trajectories and impact areas. Thus, the range which is used for a given test is flexible and can generally be tailored to meet the requirements of that test.

### E. Geography

Wallops Station is located approximately 20 miles from Pocomoke City, Maryland, near Chincoteague, Virginia. The firing sites of Wallops Station are located on Wallops Island, which is a comparatively flat, sparsely wooded, sandy island on the Atlantic coast of the Delmarva Peninsula. The latitude of the island is 37°50'N, and the longitude is 75°29'W. Wallops Station is composed of three major areas: Wallops Island, south of Chincoteague; Wallops Mainland, on the mainland behind the island; and the Main Base, west of Chincoteague. The Main Base was formerly the Chincoteague Naval Air Station, which was turned over to NASA on June 30, 1959. Figure 39 is a general map of Wallops Station which shows the location of the station with respect to Chincoteague and the main roads leading into the area. Also included in the illustration is a vicinity map which shows the relative location of Wallops Station to Washington, D. C.; Langley Field, Virginia; and Norfolk, Virginia.

F. Downrange Stations

Two sites are located about 14 miles downrange from Wallops Island near Locustville, Virginia. A combination 325- and 175-inch tracking telescope is located at one of these sites, and an IGOR telescope is installed at the other.

G. Bermuda

The Mercury Tracking Station located at Bermuda is available for limited support of Wallops Station activities. This station, when not engaged in Project Mercury support, will be able to provide downrange radar, telemetry, command-destruct, and certain real-time computing services.

H. Instrumentation

Those support facilities which are normal to the launching of a four-stage Scout vehicle will be used in the SNAP-10A Safety Flight Test, tentatively scheduled for launch during the period, April 1 to June 1, 1963.

Such facilities and instrumentation are:

1. Range Programming and Timing
2. Communications
3. Range Clearance
4. Meteorological Support
5. Data Acquisition Systems
   a. Radar Systems
   b. Telemetry Systems
   c. Photographic/Optical Systems
6. Range Safety Systems
7. Command-Destruct System
8. Data Reduction Systems
9. Support Services and Facilities

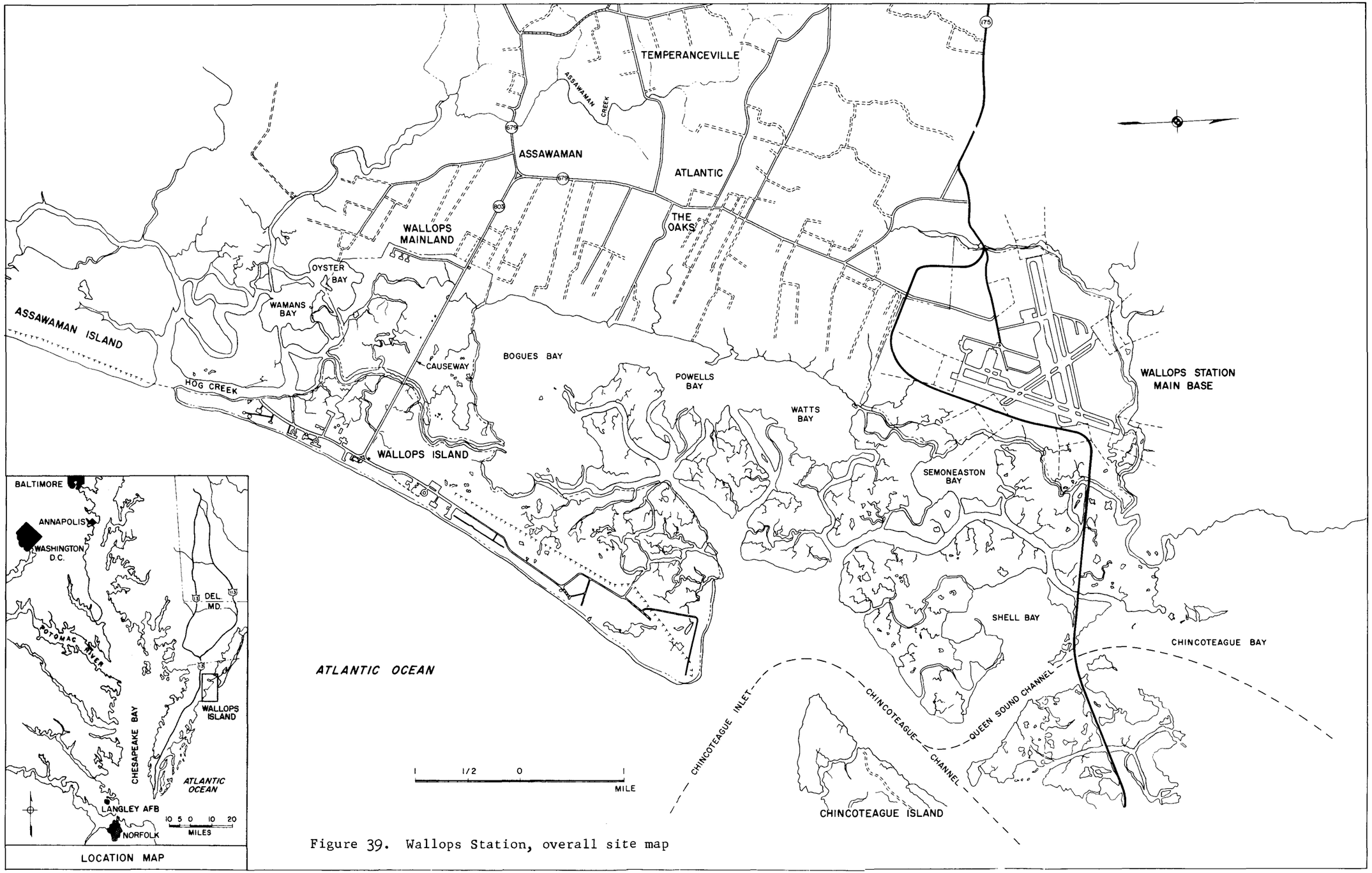


Figure 39. Wallops Station, overall site map

BLANK

## REFERENCE DOCUMENTS


1. SCDR 124-63, RFD-1 Fuel Rod Qualification Tests - Phase I.
2. Scout Users Manual, LTV Astronautics Div., 15 December 1963.
3. Nuclear Space Power Systems, Atomics International.
4. Preliminary SNAP-10A SNAPSHOT Safety Report, NAA-SR-6684, Atomics International (SRD).
5. Tentative SNAP-10A Safety Flight-Test Plan, SCDR 230-62, Sandia Corporation, (7/20/62).
6. Everhart, W. H., Flight Plan and Payload Description for SNAP-10A Safety Flight Test, SCDR 402-62, Sandia Corporation, November 1962.
7. Pre-Flight Predicted Trajectory Data, Chance-Vought Corporation, March 22, 1963.
8. Krenz, D. L., Environmental Test of SNAP-10A Safety Flight Test Vehicle, SCDR 285-63, Sandia Corporation, January 1964.
9. Flight Test Criteria for Re-entering NAP System, (Interim Report) AFSWC-TDR-62-83, November 1962.
10. Flight Test Criteria for Re-entering NAP System, Final Report, AFSWC-TDR-63-14, April 1963.

BLANK

COPY

APPENDIX

SCOUT RE-ENTRY STUDY
CONDUCTED FOR THE SANDIA CORPORATION

by

CHANCE-VOUGHT CORPORATION

29 May 1962

| Prepared by: | Checked by: | Approved by: |
|---|---|---|
| /S/ R. F. Sturgeon | /S/ J. L. Midgorden | /S/ R. H. Ross |

BLANK

COPY

SUMMARY:

A preliminary re-entry performance study for the 1962 four-stage Scout vehicle indicates that this vehicle is capable of fulfilling the mission specified by the Sandia Corporation with a minor compromise in either payload weight or velocity requirements. Replacement of the ABL-X-248 fourth-stage engine used in this study by the ABL-X-258 engine would remove the requirement of any compromise and provide the payload-velocity capabilities necessary for complete satisfaction of the mission.

INTRODUCTION:

This report releases preliminary performance data for the 1962 Scout vehicle relative to the re-entry mission defined by Purchase Order 82-3420, modified May 1, 1962, submitted by the Sandia Corporation.

Mission requirements are defined as follows:

1. A launch from Wallops Island to the vicinity of Bermuda.

2. The burnout of the final (fourth) stage should occur at an altitude of 400,000 feet with a relative flight path angle of -7 degrees and a relative velocity between 21,500 and 25,000 feet per second.

3. The payload should be at an altitude of 150,000 feet when it passes over the vicinity of Bermuda. This defines the range to be 630 nautical miles at 150,000 feet.

4. The vehicle utilized is a 1962 four-stage Scout vehicle using the Algol 2A, Castor XM-33-E5, ABL-X-259, and ABL-X-248 engines. In all cases, the latest engine data available is used.

5. Payload range is from 100 to 500 pounds.

These requirements represent a definite departure from re-entry missions previously calculated for and flown by the Scout vehicle. In the design of any trajectory, an attempt is made to allow the vehicle to follow the most efficient trajectory consistent with mission requirements. In general, the most efficient trajectory is achieved when the vehicle follows a "gravity turn" trajectory, i.e., one in which the thrust vector is always parallel to the velocity vector. Deviation of the thrust vector from the direction of the velocity vector results in reduced vehicle performance.

Since only the first three stages of the Scout vehicle are guided, the vehicle must assume an attitude before the ignition of the fourth stage that will result in the required conditions at fourth-stage burnout. This results in some loss of performance during the fourth-stage burning period, and in previous missions has been the only period during which this condition has been necessary.

The definition of this mission, however, requires a large attitude change during the second-stage coast period, before ignition of the third stage. This results in misalignment of the thrust vector with the velocity vector during both the third- and fourth-stage burning periods causing a significant velocity decrease at fourth-stage burnout. This attitude change is necessitated by the requirement that fourth-stage burnout occur at an altitude of 400,000 feet with a small relative flight path angle and that the payload descend to an altitude of 150,000 feet at a range of 630 miles. Accumulated data indicate that a payload at 400,000 feet with a relative flight path angle of -7 degrees traverses 300 nautical miles of range in descending to 150,000 feet. This requires that fourth-stage burnout occur

at a range of not greater than 330 nautical miles which necessitates the previously described attitude change, since a vehicle following a "gravity turn" trajectory to the same burnout conditions burns out at approximately 600 nautical miles.

Figure A1 illustrates the decrease in burnout velocity resulting in the procedure utilized to obtain the shorter range desired at an altitude of 150,000 feet.

RESULTS:

The data presented in the accompanying figures is obtained from trajectories programmed to meet the mission requirements. The vehicle is launched at an angle of approximately 82 degrees; this varies slightly with payload weight. After first stage burnout, the vehicle coasts to 160,000 feet and the second stage ignites. After second-stage burnout, the vehicle is programmed from the "gravity turn" trajectory which it followed to this point, by the introduction of a negative pitch angle change of approximately 60 degrees during the 25-second coast period. A constant inertial attitude is maintained through the third-stage burning period. During the 20-second coast period that follows third-stage burnout, the vehicle is pitched 17.8 degrees in the positive direction so that at fourth-stage burnout the relative flight path angle is near the required -7 degrees and the longitudinal body axis is again aligned with the velocity vector resulting in an angle of attack of zero. The payload maintains a constant inertial attitude during the descent to 150,000 feet.

Figures A3, A4, and A5 present time histories of relative velocity, altitude, range, relative flight path angle and pitch angle for payloads of 200, 400 and 600 pounds, respectively. Figures A6, A7, and A8 illustrate altitude as a function of range for the same trajectories. Figure A2 describes relative velocity at fourth-stage burnout as a function of payload for these trajectories.

CONCLUSIONS:

The data presented in these figures does not fulfill the specified conditions exactly. However, the conditions can be satisfied for a specific mission and payload. It is felt that the time required for further refinement of these trajectories is not warranted in a preliminary study. Data is presented for a relative flight path angle of -6 degrees at fourth-stage burnout because more consistent data is available for that angle than any other.

As reflected in the enclosures, the burnout velocities for the greater payload weights are somewhat lower than desired. Replacement of the ABL-X-248 fourth-stage engine used in this study by the ABL-X-258 engine would provide an increase of over 1000 feet per second in the burnout velocities described in this report. This would satisfy the velocity requirements for the heavier payloads.

Calculation of these trajectories was accomplished with a six-degree-of-freedom, three dimensional digital computer program which contains accurate simulation of the earth and its associated atmosphere and gravitational field, in addition to the physical and dynamic characteristics of the vehicle.

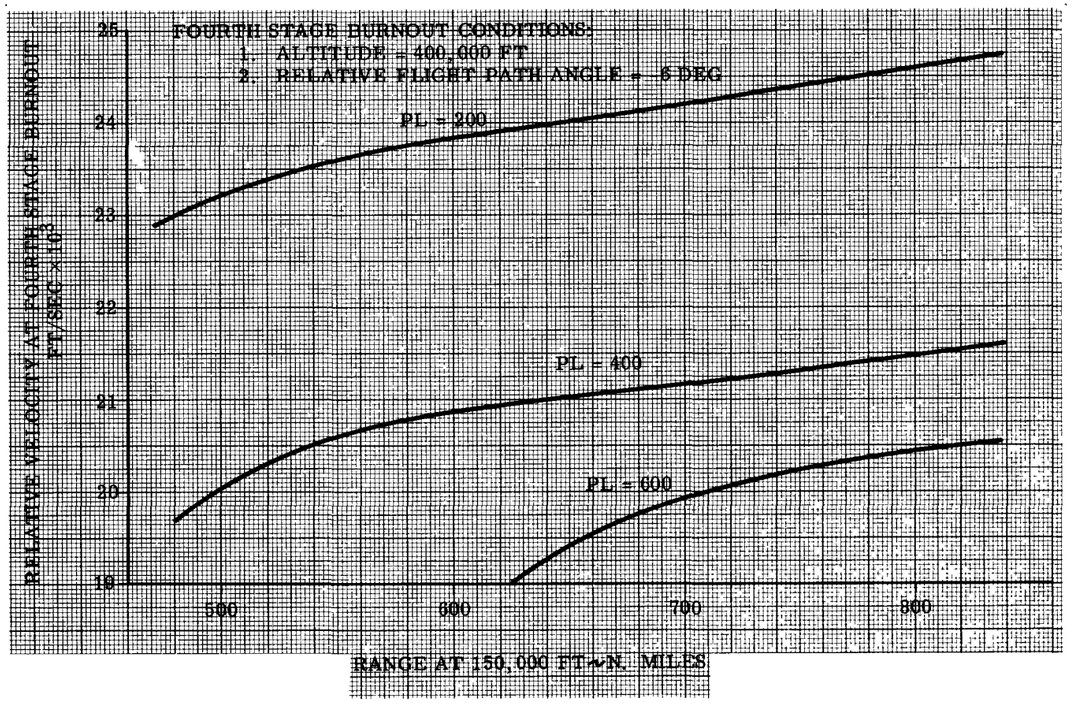


Figure A1. Sandia re-entry study, range versus relative velocity

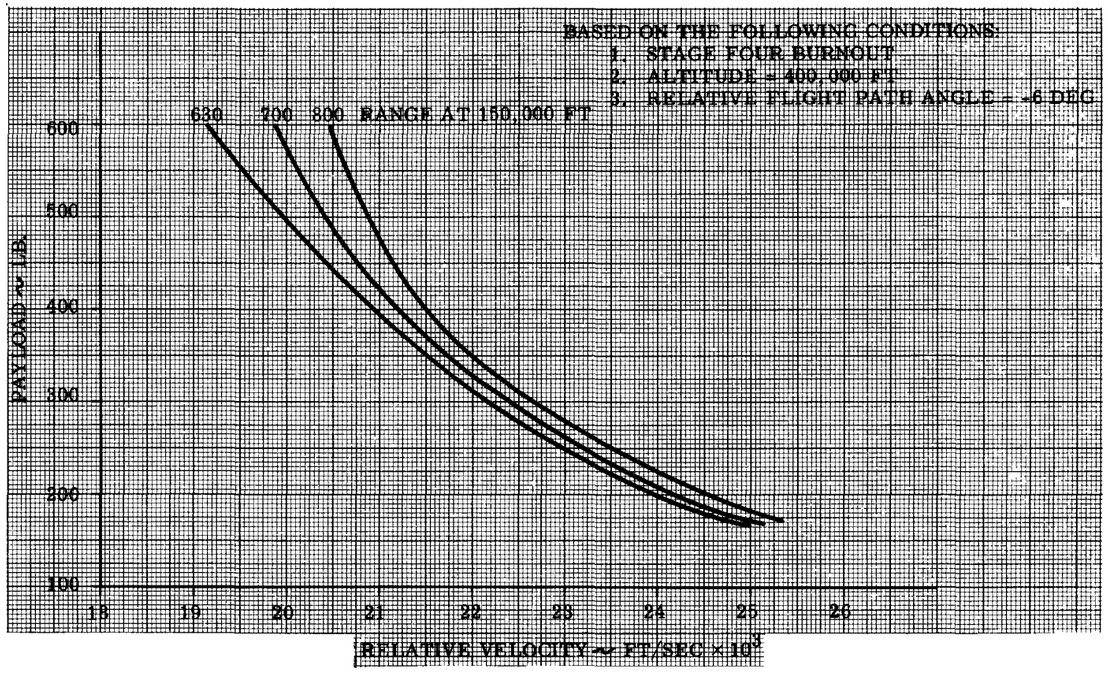


Figure A2. Sandia re-entry study, payload versus relative velocity

FIGURE A3.
SANDIA RE-ENTRY STUDY
TIME HISTORY OF FLIGHT PARAMETERS

CONDITIONS:
1. PAYLOAD = 200 LB.
2. LAUNCH SITE: WALLOPS ISLAND
3. LAUNCH ANGLE = 81.9°
4. LAUNCH AZIMUTH = 129°

VELOCITY (V)
ALTITUDE (H)
RANGE (R)
FLIGHT PATH ANGLE (γ)
PITCH ANGLE (θ)

1 B. O. 2 IGN 2 B. O. 3 IGN 3 B. O. 4 IGN 4 B. O.

PITCH ANGLE ~ DEG.
RELATIVE FLIGHT PATH ANGLE ~ DEG.
RANGE ~ N. MILES
ALTITUDE ~ FT $\times 10^{-3}$
RELATIVE VELOCITY ~ FT/SEC. $\times 10^{-3}$
TIME ~ SEC.

FIGURE A4.

SANDIA RE-ENTRY STUDY
TIME HISTORY OF FLIGHT PARAMETERS

CONDITIONS:
1. PAYLOAD = 400 LB.
2. LAUNCH SITE: WALLOPS ISLAND
3. LAUNCH ANGLE = 81.98°
4. LAUNCH AZIMUTH = 129°

VELOCITY (V)
ALTITUDE (H)
RANGE (R)
FLIGHT PATH ANGLE (γ)
PITCH ANGLE (θ)

1 B. O. 2 IGN 2 B. O. 3 IGN 3 B. O. 4 IGN 4 B. O.

PITCH ANGLE ~ DEG.
RELATIVE FLIGHT PATH ANGLE ~ DEG.
RANGE ~ N. MILES
ALTITUDE ~ FT. × $10^3$
VELOCITY ~ FT/SEC. × $10^{-3}$
TIME ~ SEC.

Figure A5.

SANDIA RE-ENTRY STUDY

TIME HISTORY OF FLIGHT PARAMETERS

1. PAYLOAD = 600 LB.
2. LAUNCH SITE: WALLOPS ISLAND
3. LAUNCH ANGLE = 82.2°
4. LAUNCH AZIMUTH = 129°

VELOCITY (V)
ALTITUDE (H)
RANGE (R)
FLIGHT PATH ANGLE (γ)
PITCH ANGLE (θ)

1 B. O. 2 IGN 2 B. O. 3 IGN 3 B. O. 4 IGN 4 B. O.

R
V
θ
H
γ

PITCH ANGLE ~ DEG: 80, 60, 40, 20, 0, -20, -40, -60

RELATIVE FLIGHT PATH ANGLE ~ DEG: 70, 60, 50, 40, 30, 20, 10, 0, -10

RANGE ~ N. MILES: 700, 600, 500, 400, 300, 200, 100, 0

ALTITUDE ~ FT $\times 10^{-3}$: 700, 600, 500, 400, 300, 200, 100, 0

RELATIVE VELOCITY ~ FT/SEC $\times 10^{-3}$: 28, 24, 20, 16, 12, 8, 4, 0

TIME ~ SEC.: 0, 40, 80, 120, 160, 200, 240, 280, 320, 360

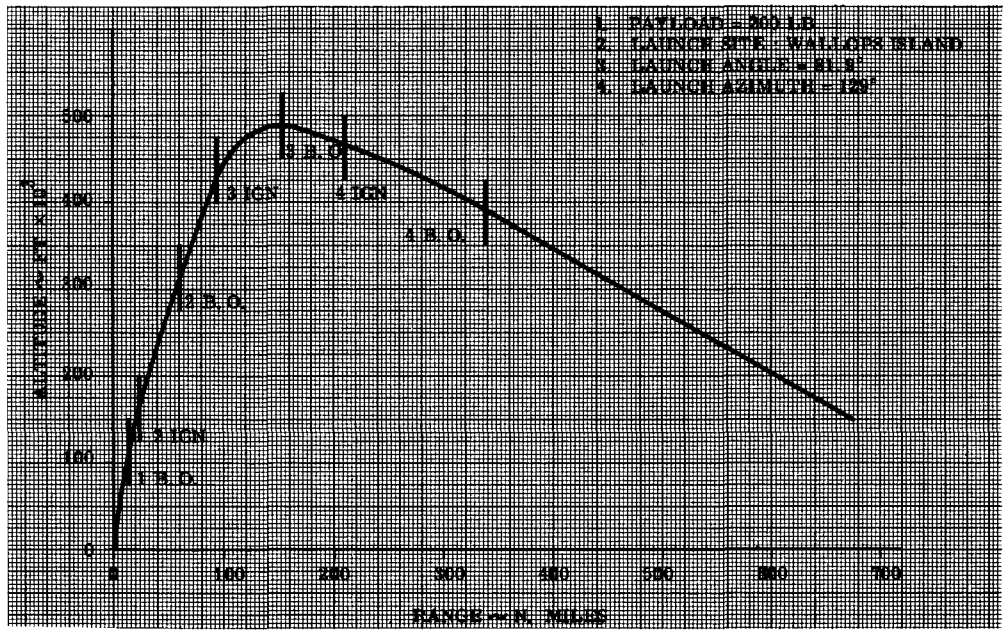


Figure A6. Sandia re-entry study, altitude versus range

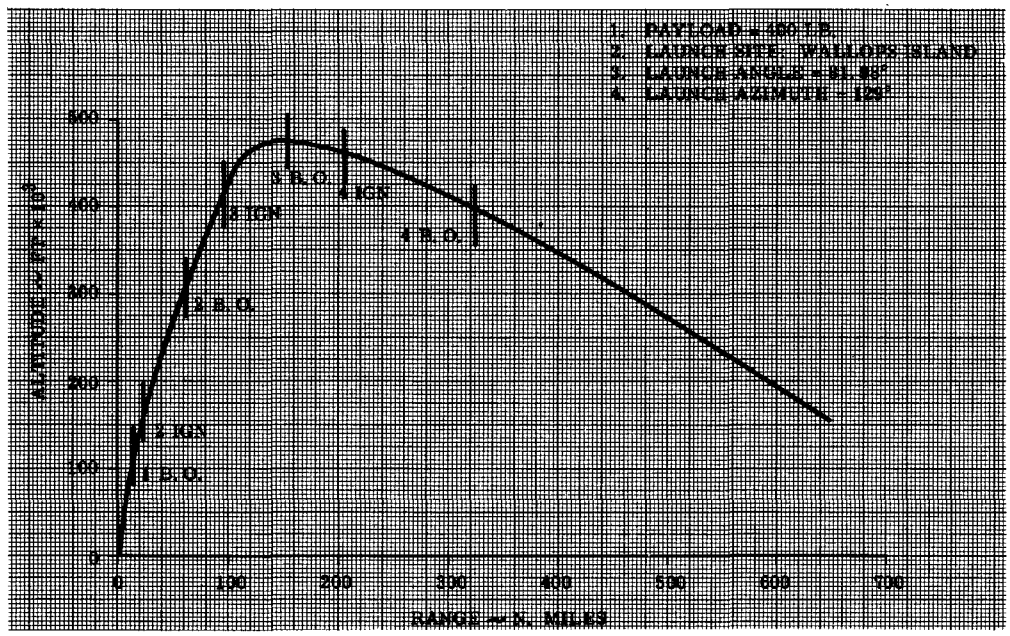


Figure A7. Sandia re-entry study, altitude versus range

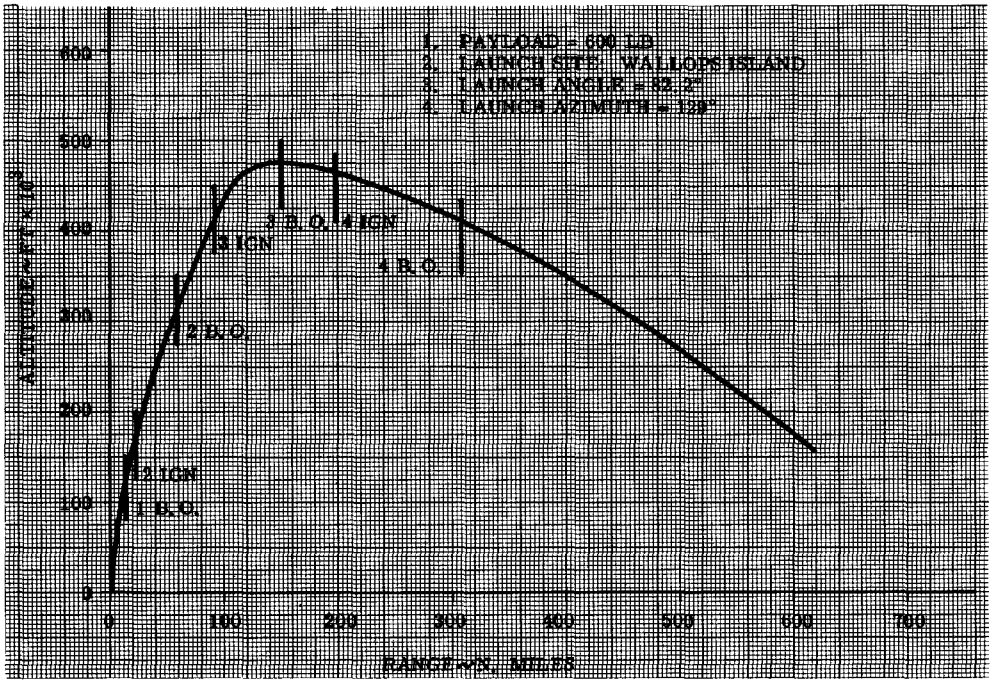


Figure A8. Sandia re-entry study, altitude versus range

DISTRIBUTION:
TID-4500 (27th Ed.), UC-36 (467)
J. A. Lieberman, Assistant Director for Nuclear Safety, Division of Reactor Development, USAEC, Washington 25, D. C.
F. K. Pittman, Director, Division of Reactor Development, USAEC, Washington 25, D.C.
H. G. Hembree, Safety Engineering & Test Branch, Division of Reactor Development, USAEC, Washington 25, D. C.
Lt. Col. W. K. Kern, Aerospace Safety Section, Engineering & Test Branch, Division of Reactor Development, USAEC, Washington 25, D. C.
R. L. Kirk, SNAP Program Director, Division of Reactor Development, USAEC, Washington 25, D. C.
Robert Lowenstein, Director, Division of Licensing & Regulation, USAEC, Washington 25, D. C.
Brig. Gen. D. L. Crowson, USAEC, Division of Military Applications, Washington 25, D. C.
W. L. Hancock, Area Manager, AEC Albuquerque Operations Office, P. O. Box 5400 Albuquerque, New Mexico (2)
S. A. Upson, Director, Reactor Operations Division, AEC Albuquerque Operations Office, P. O. Box 5400, Albuquerque, New Mexico (30)
J. V. Levy, Area Manager, USAEC, Canoga Park Area Office, P. O. Box 591, Canoga Park, California, Attn: C. A. Malmstrom (2)
I. A. Peltier, Idaho Operations Office, Idaho Falls, Idaho
C. A. Keller, USAEC, Oak Ridge Operations Office, P. O. Box E, Oak Ridge, Tennessee
T. R. Wilson, Phillips Petroleum Company, Idaho Falls, Idaho
Col. I. J. Russell, AFWL (WLRB)
Col. R. A. Gilbert, AFWL (WLG)
Lt. Col. J. W. Talley, AFWL (WLDN)
Col. D. C. Jameson, AFINS-R, KAFB
A. Glassner, Argonne National Laboratory, P. O. Box 299, Lemont, Illinois
R. L. Detterman, Atomics International, P. O. Box 309, Canoga Park, California (4)
NASA Langley Research Center, Langley Station, Hampton, Virginia, Attn: E. D. Schult (5)
T. B. Kerr, RNS, NASA Headquarters, Washington 25, D. C.
R. D. Ginter, NASA Headquarters, Washington 25, D. C.
W. A. Guild, NASA Headquarters, Washington 25, D. C.
S. P. Schwartz, 1
R. W. Henderson, 100
E. H. Draper, 1000
C. F. Bild, 1100, Attn: E. R. Frye, 1112
W. M. O'Neill, 1120
L. D. Hopkins, 1300, Attn: J. P. Cody, 1320
G. I. Hildebrandt, 1330
J. H. Findlay, 1400, Attn: J. P. Shoup, 1430
G. W. Rodgers, 1420
J. M. Wiesen, 1440
L. D. Smith, 1500, Attn: H. H. Patterson, 1530
S. A. Moore, 1540
R. A. Bice, 2000
H. E. Lenander, 2500
L. J. Heilman, 2600
J. R. Meikle, 2640
R. B. Powell, 3000
K. A. Smith, 3100
D. S. Tarbox, 3200
S. P. Bliss, 3300
M. K. Linn, 3400
C. W. Campbell, 4000
R. J. Hansen, 4200
K. S. Spoon, 4300
T. T. Robertson, 4400, Attn: F. F. Eichert, 4410
R. E. Hopper, 4500
Organization 5000
R. S. Claassen, 5100
J. W. Easley, 5300
T. B. Cook, 5400, Attn: B. F. Murphey, 5410

DISTRIBUTION (cont)
J. D. Shreve, 5414
F. C. Cheston, 6000
G. A. Fowler, 7000
L. E. Hollingsworth, 7200, Attn: H. E. Viney, 7210
W. T. Moffat, 7220, Attn: R. N. Browne, 7224
D. Beatson, 7223-5
G. E. Hansche, 7240
J. C. Eckhart, 7250
W. A. Gardner, 7300/7310
R. H. Schultz, 7320
J. W. Pearce, 7330
D. B. Shuster, 7400
V. E. Blake, 7410
H. E. Hansen, 7411 (6)
I. B. White, 7411
A. J. Clark, Jr., 7412 (6)
J. Jacobs, 7412-2
J. I. Hegge, 7412-2
R. D. Klett, 7412-2
H. R. Spahr, 7412-2
H. K. Togami, 7412-2
A. E. Bentz, 7413 (6)
C. E. Erickson, 7413-1
A. Y. Pope, 7420
J. H. Scott, 7430
W. C. Scrivner, 7600, Attn: J. L. Tischhauser, 7620
B. S. Biggs, 8000
L. Gutierrez, 8100
W. A. Jamieson, 8232
D. R. Cotter, 9100
B. R. Allen, 3421
R. C. Smelich, 3427-3 (50)
M. G. Randle, 3428-1, Bldg. 836
M. G. Randle, 3428-1, Bldg. 880
J. M. Zanetti, 3412